

Crustal Contamination and Fluid–Rock Interaction during the Formation of the Platreef, Northern Limb of the Bushveld Complex, South Africa

CHRIS HARRIS* AND JEFFERSON B. CHAUMBA

DEPARTMENT OF GEOLOGICAL SCIENCES, UNIVERSITY OF CAPE TOWN, RONDEBOSCH 7700, SOUTH AFRICA

RECEIVED MARCH 20, 2000; REVISED TYPESCRIPT ACCEPTED DECEMBER 5, 2000

The Platreef is the main platinum group element (PGE)-bearing facies of the northern limb of the Bushveld complex, but unlike the Merensky Reef of the eastern and western limbs, it is in direct contact with the country rock. Mineral separate $\delta^{18}\text{O}$ values for samples from the Upper Zone and Main Zone of the northern limb indicate crystallization from a well-mixed, already contaminated, magma having a $\delta^{18}\text{O}$ value of 7.5‰. Pyroxenes from the pyroxenites facies of the Platreef at Sandsloot Mine have $\delta^{18}\text{O}$ values that are up to 2.4‰ higher than pyroxenes from the Upper and Main Zones. These differences can be explained by additional assimilation of up to 18% dolomite, which is in contact with the intrusion at this locality. Samples from the Platreef that have plagioclase and pyroxene not in oxygen isotope equilibrium appear to have interacted with fluids during slow cooling. Quartz veins with granophyric margins have $\delta^{18}\text{O}$ values between 10.1 and 12.2‰, which suggest that the fluid that passed through the cooling Platreef had a $\delta^{18}\text{O}$ value of 7–9‰. These data, together with hydrogen isotope data from minerals and whole-rock samples (δD of biotite – 60 to – 88‰) of the Platreef suggest interaction with magmatic fluid at low water/rock ratios. Interaction of this fluid with the calcisilicate footwall rocks lowered their $\delta^{18}\text{O}$ values.

KEY WORDS: *Bushveld complex; Platreef; stable isotopes; crustal contamination; fluid–rock interaction*

INTRODUCTION

The mafic component of the 2050 Ma Bushveld complex of South Africa is the largest igneous intrusion on Earth

and contains some of the most important magmatic ore deposits yet discovered. The intrusion covers an area of roughly 65 000 km² (e.g. Tankard *et al.*, 1982) and lies almost entirely within the bounds of the Transvaal Basin (Fig. 1). The layered igneous rocks (the Rustenburg Layered Suite, SACS, 1980) can be divided into eastern and western limbs of approximately the same size, and a smaller northern limb. The northern limb differs in several important aspects from the more well-known eastern and western limbs (e.g. Van der Merwe, 1976; Buchanan *et al.*, 1981; Cawthorn *et al.*, 1985; Eales & Cawthorn, 1996). First, the layered rocks show a pronounced transgression across the floor rocks from a level above the Magaliesberg Quartzite Formation south of the town of Potgietersrus, across the whole Pretoria Group, and the banded iron formations and dolomites of the older Chuniespoort Group, onto Archaean granitic rocks (Fig. 1). Second, the igneous layering shows an apparent transgressive relationship with respect to the contact, such that ultramafic rocks of the Lower Zone abut against the contact south of Potgietersrus, whereas to the north, rocks forming the base of the intrusion are progressively higher in the stratigraphic succession of the intrusion. Third, although the major platinum group element (PGE) mineralized horizon of the northern limb (the Platreef) bears some petrographic resemblance to the Merensky Reef at the top of the Critical Zone of the eastern and western limbs, it is situated at the base of the layered rocks and the mineralized zone is much thicker (Gain & Mostert, 1982).

*Corresponding author. Present address: Département de Géologie, Université Jean Monnet, 23 rue Paul Michelon, F-42023 Saint Étienne Cédex 2, France. E-mail:

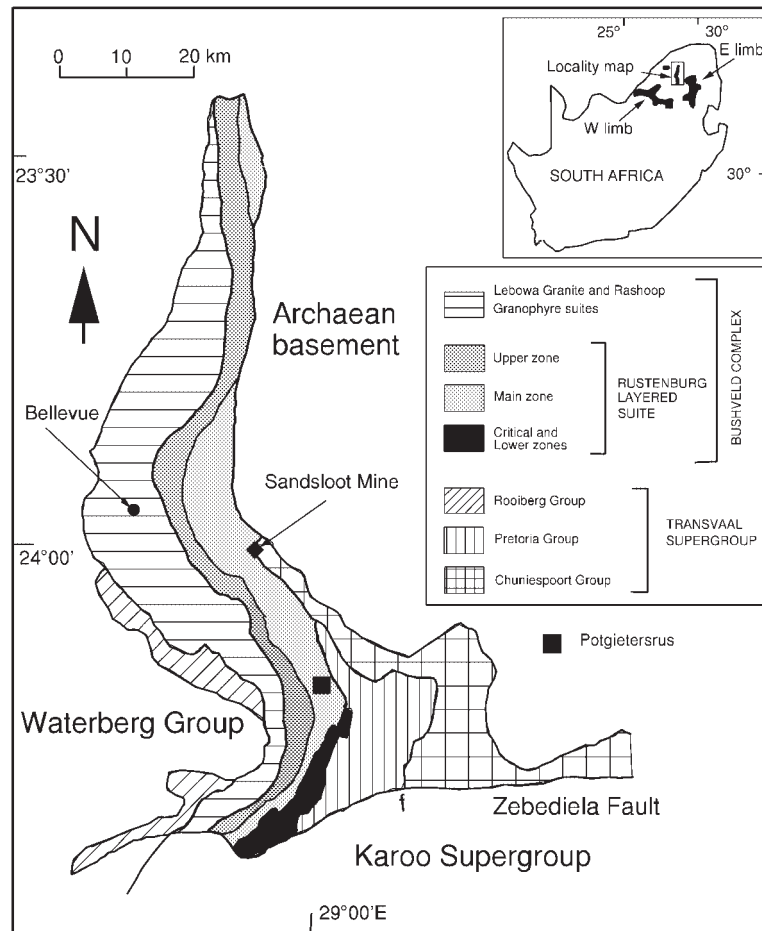


Fig. 1. Sketch map of northern limb of the Bushveld complex. The location of the Potgietersrus Platinum Mine at Sandsloot and the Bellevue borehole are shown. The inset map shows the outcrop of the Rustenburg Layered Suite in southern Africa.

The Platreef has been described in detail by Gain & Mostert (1982) and Lee (1996), who considered it to be part of the Critical Zone, which is only poorly developed in the northern limb to the south of Potgietersrus. The Platreef consists of a complex series of medium- to coarse-grained pyroxenites and norites, which contains xenoliths of the floor rocks. Mineralization of Ni, Cu and PGE is sporadic but occurs over a zone up to 200 m in width (Gain & Mostert, 1982). The Platreef north of Potgietersrus has been mined for platinum (and other base metals) intermittently since 1926 (Wagner, 1925; Buchanan *et al.*, 1981). In 1993 mining operations using open pit methods started at the Sandsloot Mine operated by Potgietersrus Platinum Mines Limited, ~30 km NW of the town of Potgietersrus.

PURPOSE OF STUDY

The mineralization of the Merensky Reef of the main Bushveld intrusion is generally thought to be of magmatic

origin with some evidence for fluid involvement but little or no evidence for significant effects of fluid on grade of mineralization (e.g. Barnes & Campbell, 1988; Schiffries & Rye, 1989, 1990; Reid *et al.*, 1993). The Platreef, however, shows considerably more visual evidence for post-magmatic fluid interaction. In addition, the situation of the Platreef, in direct contact with the country rock, means that wall-rock assimilation has been suggested as being especially important in the origin and mineralization of the basal part of the northern limb (Buchanan *et al.*, 1981; Cawthorn *et al.*, 1985; Barton *et al.*, 1986).

One of the most interesting geochemical features of the Rustenburg Layered Suite in the eastern and western limbs is the isotope evidence for contamination (e.g. Harmer & Sharpe, 1985; Schiffries & Rye, 1989). Initial Sr-isotope ratios vary with stratigraphic height and change suddenly at certain stratigraphic horizons (e.g. the Merensky Reef; Kruger & Marsh, 1982). These variations have been interpreted by various workers as

being caused by the sudden influx of magma of distinctly different isotope composition. The δO values of Bushveld magmas estimated from mineral $\delta^{18}\text{O}$ values are typically $\sim 1\%$ higher than expected for a mantle-derived basaltic magma (Schiffries & Rye, 1989). In contrast to the behaviour of Sr-isotopes, the oxygen isotope data show no systematic change with stratigraphic height, which is consistent with the parental magmas assimilating a significant amount of crust before emplacement.

The Platreef is important as a source of platinum group elements (e.g. Lee, 1996). There has been much debate in the recent literature on the origin of platiniferous 'reefs' (e.g. Ballhaus & Stumpff, 1986; Barnes & Campbell, 1988; Boudreau & McCallum, 1992), in particular concerning the role of fluids. The present paper has two major aims. The first is to compare the oxygen isotope composition of the northern limb of the Bushveld with previously published data (Schiffries & Rye, 1989) from the eastern and western limbs of the intrusion. It is important to establish whether or not the northern limb shares the unusual O-isotope character of the main intrusion. To make the comparison, we have analysed samples from a 2500 m core recovered from drilling through the northern limb on the farm Bellevue (Fig. 1). The second aim is to determine the role of crustal contamination in the formation of the Platreef, and to assess the subsequent role of fluid-rock interaction. Our study of the Platreef is based on samples collected at Sandsloot (Fig. 1), the site of the largest platinum mine on the Platreef. The main analytical tool employed has been stable (O, H and C) and Sr isotopes, which are particularly useful in understanding the processes of crustal contamination and fluid-rock interaction (e.g. Gregory & Taylor, 1981; Gregory & Criss, 1986; Taylor & Sheppard, 1986; Gregory *et al.*, 1989). A study of the mineralization of the Platreef is beyond the scope of this paper and will be presented elsewhere.

GEOLOGY

The geology of the Bellevue core has been described by Knoper & von Gruenewaldt (1992) and is not described in detail here. The boundary between the Main Zone and the Upper Zone was intersected at ~ 1580 m, but the core does not extend as far as the Platreef. The samples are the same as those analysed by Ashwal & Hart (1995) and were taken from plagioclase-rich horizons. The geology of the opencast mine at Sandsloot at the time of sampling, in May 1995, is shown in Fig. 2. The mine then consisted of two pits, the Main Pit and the Satellite Pit. The width of the mineralized zone (the Platreef) in the Main Pit thinned to the north and also downwards. Three sample traverses were made across the Platreef at levels ('bench') 14, 16 and 20. The detailed

geology of the bench 20 traverse is shown in Fig. 2, and the essential features of the geology are the same in the other two traverses.

The Platreef reaches a maximum thickness of 250 m over the northern limb as a whole, and consists of an assemblage of pyroxenites, melanorites, norites, xenoliths and fragments of dolomite (Van der Merwe, 1976; Gain & Mostert, 1982). At Sandsloot Mine, the Platreef is in contact with the dolomite and forms a unit up to ~ 65 m thick. The part of the Platreef in contact with the dolomite is termed 'parapyroxenite' by the mine geologists and denotes a highly altered rock, of variable thickness, which is possibly a mechanical mixture of calcsilicate material (metamorphosed and metasomatized dolomite), pyroxene-rich igneous rocks, and minor serpentinite. This is followed by a 'pyroxenite' unit, which on account of its generally $>10\%$ plagioclase content should properly be termed a pyroxene-rich gabbro (e.g. Le Maitre, 1989). This is followed by the norites of the Main Zone of the intrusion. In this paper we will use the nomenclature in common usage at the mine, namely, norite, pyroxenite and parapyroxenite. The mineralized zone (the Platreef) is generally confined to the pyroxenite and parapyroxenite units (Fig. 2). The boundary between the parapyroxenite and the country rock is impossible to locate; in this paper the term calcsilicate is used only for samples that demonstrably come from the country rock.

The youngest igneous rock at Sandsloot is a ferrogabbro dyke exposed in the wall of the pit about 50 m to the west of the bench 20 traverse (Fig. 2). This dyke might be related to the subsequent intrusion of the Upper Zone (C. A. Lee, personal communication, 1999). Also present are a number of veins up to ~ 1 m in thickness. These consist of massive quartz interiors with 20–30 cm thick granophyric margins which presumably indicate relatively high temperatures of formation. The core of one vein (PP10) contains minor amounts of calcite. Three such veins cut the bench 20 traverse (Fig. 2).

PETROGRAPHY

The petrography and mineral chemistry of samples analysed from the Bellevue core (Fig. 1) have already been described by Knoper & von Gruenewaldt (1992) and Ashwal & Hart (1995). The following is a generalized description of the changes in petrography passing from the hanging-wall norite, through the mineralized Platreef to the contact with the calcsilicates and encompasses all the petrographic features of the three sample traverses at Sandsloot (Fig. 2).

The norites are coarse grained with maximum grain size of ~ 5 mm and contain primocrysts of plagioclase and orthopyroxene. The freshest samples contain

traverse consists almost entirely of clinopyroxene (e.g. sample PP17; see Table 2, below) and appears to be a reaction rim around a calcsilicate xenolith. Given that clinopyroxene and olivine are common constituents of the parapyroxenite, but are not found in the overlying pyroxenite, it seems likely that the parapyroxenites consist mostly of transformed dolomite floor rocks.

The ferrogabbro, which intrudes the norite, west of the bench 20 traverse (Fig. 2), is one of the freshest rock-types exposed at Sandsloot and contains 50% pyroxene (dominantly orthopyroxene), 40–45% plagioclase and 5–10% opaque oxide. This rock is finer grained than the main gabbro types, with an average grain size of ~1–2 mm. The granophyric margins of the quartz veins that cut the Platreef consist almost entirely of intergrown albite and quartz. Biotite, which is partially replaced by chlorite, is the only other mineral present (<5 modal %).

The sulphide minerals were not studied in detail during this work, but appear to be similar to those identified in the Platreef 10 km north of Sandsloot by Gain & Mostert (1982). The major sulphide minerals present are pyrrhotite, pentlandite, chalcopyrite and pyrite, which are heterogeneously distributed as crystals of up to 1 cm diameter throughout the mineralized zone (Fig. 2). The maximum sulphur content in the analysed samples was 9308 ppm, which is equivalent to ~2.7 wt % sulphide.

ANALYTICAL METHODS

All data were obtained at the University of Cape Town (UCT). Mineral chemical data were determined using a wavelength-dispersive Cameca microprobe and whole-rock chemical analyses were made using standard X-ray fluorescence (XRF) methods (e.g. Duncan *et al.*, 1984). Major elements, with the exception of Na, were determined on fusion discs, and trace elements and Na were determined on 6 g powder briquettes.

All stable isotope ratios were measured using a Finnigan MAT 252 mass spectrometer and are reported in the familiar δ notation where $\delta = (R_{\text{sample}}/R_{\text{standard}} - 1) \times 1000$ and $R = {}^{18}\text{O}/{}^{16}\text{O}$, D/H or ${}^{13}\text{C}/{}^{12}\text{C}$. Oxygen isotope data for whole rocks and silicate minerals were obtained by conventional methods using ClF_3 as the reagent (Borthwick & Harmon, 1982). Further details of the extraction methods for oxygen from silicates employed at UCT have been given by Vennemann & Smith (1990) and Harris & Erlank (1992). The quartz standard NBS-28 was analysed in duplicate along with eight samples and data were normalized to the SMOW scale using the value of 9.64‰ recommended by Coplen *et al.* (1983). The average mean deviation of 12 duplicate NBS-28 quartz standard analyses was 0.10‰. Hydrogen was produced from about 30 mg of biotite and 100 mg of whole rock by the method of Venneman & O'Neil (1993),

with 'Indiana' Zn being used to reduce the water to H_2 . The amount of Zn was about five times that normally required to reduce the water to prevent 'poisoning' of the Zn by any fluorine that might be liberated from the minerals. For hydrogen, an internal water standard (CTMP, $\delta\text{D} = -9\text{‰}$) was used to calibrate the data to the SMOW scale and the data were normalized so that SLAP gave a value of -428‰ on the SMOW scale, as recommended by Coplen *et al.* (1983). Water contents of minerals and whole rocks were estimated from the voltage measured on the mass two collector on the mass spectrometer, as described by Venneman & O'Neil (1993). The carbon and oxygen isotope ratios of carbonate minerals were determined on CO_2 produced by reaction of whole-rock powders with '103%' phosphoric acid (McCrea, 1950). Samples were reacted overnight at 50°C and analyses are of the total carbonate present. The dominant carbonate mineral present was calcite, hence the calcite–phosphoric acid fractionation factor (1.009) was used in the correction procedure. Data were normalized to the SMOW and PDB scales, respectively, using an internal standard calibrated against NBS-19 ($\delta^{18}\text{O} 28.64\text{‰}$, $\delta^{13}\text{C} 1.95\text{‰}$). Graphite was analysed using an on-line continuous flow device.

The Sr-isotope data were obtained using a VG Sector multi-collector mass spectrometer in dynamic mode, following conventional ion-exchange separation. To correct for mass fractionation effects, measured ${}^{87}\text{Sr}/{}^{86}\text{Sr}$ ratios were normalized such that ${}^{86}\text{Sr}/{}^{88}\text{Sr} = 0.1194$. Three analyses of NBS-987 made during the course of this work gave ${}^{87}\text{Sr}/{}^{86}\text{Sr}$ ratios of 0.710239(10), 0.710279(11) and 0.710239(9), where the figures in parentheses are the standard errors for repeated measurements of the isotope ratio and relate to the least significant digit(s).

MINERAL CHEMISTRY

Pyroxene analyses from selected samples of norite (PP3), pyroxenite (PP8) and several samples of parapyroxenite (PP17, PP20, PP33 and PP49) are presented in Table 1 and plotted on the pyroxene quadrilateral in Fig. 3. It should be noted that the norite contains both clinopyroxene and orthopyroxene whereas the pyroxenite contains only orthopyroxene. The orthopyroxene in the pyroxenite is slightly less magnesian than that of the norite. The parapyroxenites contain only clinopyroxene, but these are distinctly more calcic than clinopyroxene in the norite. Although some analyses plot above the Di–Hd join (Fig. 3), this is due to the presence of Al in octahedral sites and Ca does not exceed one cation per six oxygens (Table 1). Clinopyroxenes in parapyroxenite sample PP20 are notable for their high Al content (up to 8.75 wt % or 0.38 p.f.u., Table 1). The higher Ca content of parapyroxenite clinopyroxenes compared with those

Table 2: Major element data for selected samples

Sample:	PP1	PP2	PP3	PP4	PP5	PP7	PP8	PP9	PP11	PP12	PP13	PP14	PP15	PP16	PP17	PP18
Type:	N	N	N	V	N	P	P	P	P	P	PP	PP	PP	PP	PP	PP
SiO ₂	50.37	50.95	51.35	72.31	51.78	52.99	51.69	53.18	52.39	51.55	40.22	43.22	46.29	40.00	48.26	51.82
TiO ₂	0.20	0.18	0.17	0.15	0.17	0.30	0.23	0.22	0.19	0.24	0.22	0.22	0.23	0.20	0.27	0.13
Al ₂ O ₃	21.51	18.90	17.17	12.81	16.80	5.97	4.00	5.18	7.19	6.67	3.62	5.77	6.14	8.32	4.72	1.32
FeO	4.87	6.73	7.47	1.84	7.61	12.53	12.64	11.26	10.14	11.32	12.35	7.47	6.74	8.13	6.70	4.25
MnO	0.10	0.13	0.14	0.03	0.14	0.22	0.23	0.22	0.19	0.20	0.31	0.44	0.26	0.46	0.31	0.41
MgO	5.43	8.03	10.04	1.44	10.56	19.03	21.86	22.34	20.90	20.08	29.78	23.10	18.69	24.63	13.61	16.03
CaO	11.39	10.63	10.41	2.98	10.19	5.04	3.89	4.19	6.46	7.27	4.36	13.35	17.50	10.82	24.08	24.86
Na ₂ O	2.37	2.11	2.03	6.47	1.95	0.86	0.31	0.61	0.86	0.66	b.d.	0.14	0.15	0.02	0.05	0.03
K ₂ O	1.06	0.68	0.20	0.20	0.21	0.21	0.27	0.17	0.23	0.28	0.08	0.12	0.21	0.10	0.21	0.02
P ₂ O ₅	0.04	0.02	0.02	0.05	0.02	0.03	0.14	0.02	0.02	0.03	0.02	0.02	0.03	0.02	0.05	0.02
H ₂ O ⁻	0.05	0.04	0.25	0.10	0.05	0.05	0.22	0.27	0.15	0.04	0.41	0.27	0.22	0.27	0.08	0.04
LOI	2.70	1.75	1.20	1.93	1.52	2.69	2.27	0.37	1.68	1.69	8.5	5.54	3.97	7.30	1.86	0.80
Total	100.09	100.13	100.52	100.3	100.99	99.99	99.36	100.02	100.38	100.03	99.86	99.62	100.41	100.26	100.00	99.73
Nb	1	b.d.	b.d.	15	1	3	1	1	1	1	1	1	1	1	1	1
Zr	15	10	10	78	9	30	17	17	15	16	21	22	22	28	23	23
Y	6	6	5	23	5	10	7	6	6	7	4	7	7	6	7	3
Sr	333	263	214	65	198	57	34	48	119	141	16	42	20	49	6	10
U	b.d.	1	2	7	1	1	b.d.	b.d.	1	2	2	1	b.d.	1	1	b.d.
Rb	36	23	5	11	6	12	12	9	7	6	5	6	13	4	2	3
Th	2	b.d.	1	10	0	2	2	1	b.d.	3	1	1	b.d.	1	2	2
Pb	5	1	2	10	1	5	10	11	4	12	15	20	6	6	5	50
S	36	177	112	46	45	1866	2611	662	2715	4755	2732	3051	855	1078	4571	3358
Zn	40	56	60	20	61	104	69	102	72	80	56	52	53	114	47	63
Cu	23	46	42	30	39	657	436	348	1206	2357	1119	1351	423	291	1108	778
Ni	114	189	239	58	258	1921	1260	1481	2991	3848	2838	3057	819	889	2148	1927
Co	32	46	53	11	57	109	108	95	113	131	146	80	56	56	64	41
Cr	311	417	656	69	717	1858	2715	2871	2459	1657	572	78	410	92	40	12
V	92	115	125	36	127	182	174	163	143	153	86	91	137	78	160	44
Ba	211	182	75	32	75	40	32	37	80	103	29	59	28	30	7	n.d.
Sc	20	24	25	9	26	35	36	33	29	31	18	24	35	20	23	8

of the norites and pyroxenites suggests that the former are of metamorphic origin [also recognized by Buchanan *et al.* (1981)]. The ferrogabbro that cuts the norite near the traverse of bench 20 (Fig. 3) contains pyroxenes that are considerably more iron rich (typical *mg*-number for opx 0.51, for cpx 0.40) than those of the norite (*mg*-number for opx 0.80–0.83), consistent with a relative of the Upper Zone.

Olivine analyses were made only for sample PP20 (a parapyroxenite) where olivine is present as cores to serpentine. Olivine in this rock shows a restricted range in composition, averaging Fo₈₄ (Fig. 3; Table 1), which

is consistent with either a magmatic or metamorphic origin. Given that olivine is absent in the pyroxenites, it is more likely that olivine in the parapyroxenites is of metamorphic origin.

The norite sample (PP3) contains cumulus plagioclase of fairly restricted composition (An_{70–66}), which is slightly more calcic than the intercumulus plagioclase (An_{65–62}) in the pyroxenite sample (PP8). The ferrogabbro dyke contains rather more sodic plagioclase (An_{64–45}). The plagioclase in both the norites and pyroxenites is more calcic than in samples of Platreef in contact with Archaean granite (An_{30–60}; Cawthorn *et al.*, 1985).

Table 2: continued

Sample:	PP19	PP20	PP21	PP22	PP23	PP24	PP25	PP26	PP31	PP32	PP33	PP34	PP42	PP53	PP67
Type:	PP	PP	CS	CS	N	FG	GV	N	CS	CS	PP	CS	PP	P	G
SiO ₂	52.48	46.52	32.29	35.06	51.18	51.24	70.49	49.39	38.68	38.84	42.81	35.30	39.15	45.44	72.11
TiO ₂	0.19	0.60	0.20	0.05	0.17	0.22	0.12	0.22	0.07	0.07	0.65	0.11	0.22	0.54	0.15
Al ₂ O ₃	7.21	6.40	8.99	4.41	7.11	23.62	11.35	22.82	2.17	3.22	6.59	8.65	3.48	7.52	12.77
FeO	10.13	6.05	6.53	3.60	9.79	3.99	5.34	3.87	5.97	7.83	5.18	6.75	15.18	5.18	1.84
MnO	0.19	0.49	2.74	0.57	0.20	0.08	0.06	0.08	0.92	0.41	0.20	0.77	0.21	0.32	0.03
MgO	20.92	15.71	24.95	21.63	21.72	4.69	2.48	4.52	25.07	26.99	12.92	25.98	23.67	15.31	1.45
CaO	6.46	21.58	11.99	25.61	6.66	11.96	1.32	11.58	17.06	12.55	27.36	11.77	7.22	21.82	2.98
Na ₂ O	0.09	0.10	b.d.	b.d.	0.66	1.98	4.52	2.72	b.d.	b.d.	0.03	b.d.	0.05	0.12	6.47
K ₂ O	0.23	0.03	b.d.	0.01	0.15	0.88	0.24	0.85	b.d.	0.01	0.07	b.d.	0.06	0.04	0.20
P ₂ O ₅	0.02	0.02	0.02	0.02	0.02	0.06	0.04	0.06	0.02	0.02	0.03	0.02	0.02	0.03	0.05
H ₂ O ⁻	0.15	0.19	0.68	1.45	0.61	0.09	0.56	0.47	0.74	0.59	0.04	0.13	0.86	0.18	0.10
LOI	1.68	2.60	10.31	8.08	2.38	0.44	2.34	2.20	9.86	10.12	5.20	10.75	8.12	2.85	1.93
Total	99.75	100.29	98.70	100.49	100.64	99.25	98.85	98.77	100.56	100.65	100.54	100.2	98.22	99.34	99.48
Nb	1	1	b.d.	1	1	4	3	1	b.d.	b.d.	2	b.d.	b.d.	1	7
Zr	23	76	5	2	11	26	160	23	3	2	109	3	14	92	144
Y	8	13	15	4	4	24	11	7	11	13	10	7	4	12	12
Sr	6	15	2	14	53	204	53	278	2	2	32	2	12	20	375
U	b.d.	b.d.	b.d.	b.d.	1	b.d.	13	1	b.d.	2	b.d.	b.d.	b.d.	1	3
Rb	19	2	b.d.	b.d.	6	2	16	30	1	b.d.	4	b.d.	3	1	118
Th	b.d.	2	b.d.	2	3	b.d.	41	1	1	1	b.d.	b.d.	b.d.	3	9
Pb	9	28	36	1	3	b.d.	24	3	2	3	2	b.d.	7	25	18
S	9308	4841	6064	446	204	1583	38	47	202	307	416	593	5064	2930	9
Zn	81	43	71	21	76	98	23	32	7	8	17	48	65	22	52
Cu	1285	1019	1126	50	104	114	6	27	6	176	190	117	1201	2348	8
Ni	2866	1602	465	228	739	53	12	109	243	405	172	357	2305	3261	19
Co	64	38	11	23	85	100	12	24	35	44	33	45	148	51	5
Cr	26	38	34	12	2318	49	22	283	61	170	103	893	7798	60	32
V	69	62	10	b.d.	142	1021	11	84	6	9	265	30	104	81	17
Ba	9	10	b.d.	b.d.	48	84	34	236	b.d.	b.d.	15	b.d.	16	15	1011
Sc	17	18	5	9	30	65	5	19	12	15	45	10	19	21	4

Symbols for rock types as for Table 1 except: GV, granophyric margin of quartz/granophyre vein; G, Archaean granite 3 km from mine. b.d., below detection.

WHOLE-ROCK GEOCHEMISTRY

Interelement variations

Chemical analyses of selected rocks are given in Table 2, and selected major element oxides vs SiO₂ and MgO are shown in Fig. 4. The most important feature to note is that the norites, pyroxenites and the ferrogabbro (i.e. the magmatic rocks) show coherent variations. Because these rocks are cumulates the chemical variation is controlled largely by modal mineralogy. In the oxide vs MgO and SiO₂ plots (Fig. 4), the norite and pyroxenites plot between typical plagioclase and orthopyroxene compositions, which indicates that varying proportions of

these two minerals are the dominant control on whole-rock composition.

Data for parapyroxenites and footwall calcsilicates are also plotted in Fig. 4. They show considerably less coherent variation than the pyroxenites and norites (Fig. 4), having lower SiO₂ (<50 wt %), FeO and Na₂O contents, and higher CaO contents. By comparison with the parapyroxenites, the calcsilicates have lower SiO₂ (<40 wt %), lower FeO/MgO and higher CaO/MgO. The high CaO and the low sodium content of the parapyroxenites are consistent with a metamorphic origin. The calcsilicates have lower SiO₂ and higher CaO/MgO than the parapyroxenites, which suggests that they

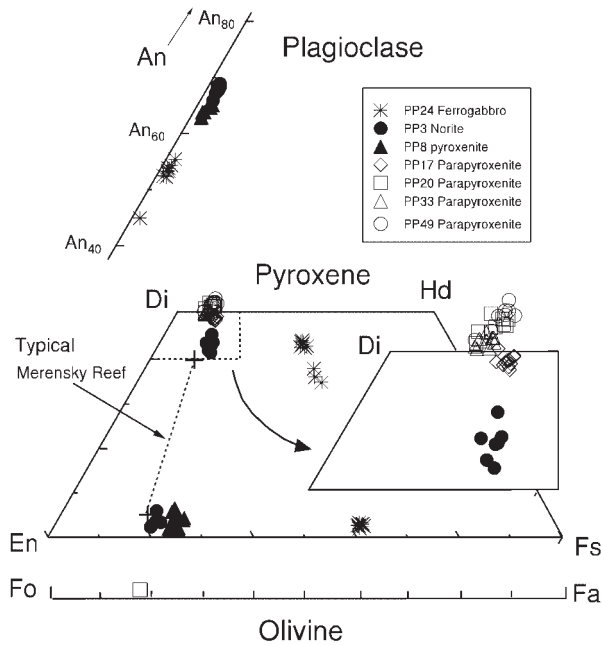


Fig. 3. Variation in composition of plagioclase, pyroxene and olivine in samples from and adjacent to the Platreef at Sandsloot. Composition of typical Merensky Reef pyroxenes from Cawthorn *et al.* (1985).

contain a higher component of dolomite. The high (up to 9 wt %) Al_2O_3 content of two of the calcsilicate samples appears to be due to a high content of sheet silicate alteration minerals, and the high Al_2O_3 content of the clinopyroxenes (Table 1).

Because the pyroxenes and norites are cumulate rocks, they have very low abundances of the immobile incompatible trace elements such as Zr, Nb and Y (e.g. <20 ppm Zr, Table 2). In Fig. 5, various trace elements are plotted against SiO_2 and MgO. The norites show a systematic decrease in Cr and Ni with decreasing MgO. The pyroxenites show a systematic decrease in Cr with decreasing MgO, but Ni shows no systematic variation with MgO. Both the norites and the pyroxenites show a systematic increase in Ba and Sr content with increasing SiO_2 . These variations are qualitatively consistent with variation in pyroxene and plagioclase content.

The parapyroxenites and calcsilicates show no systematic variations in trace element content with SiO_2 and MgO (Fig. 5). Both the parapyroxenites and calcsilicates have consistently low Ba and Sr content and, apart from one sample, low Cr contents (<2000 ppm). This is consistent with a non-magmatic origin for the abundant clinopyroxene in the parapyroxenites. The Ni content of the parapyroxenites is much higher than that of the

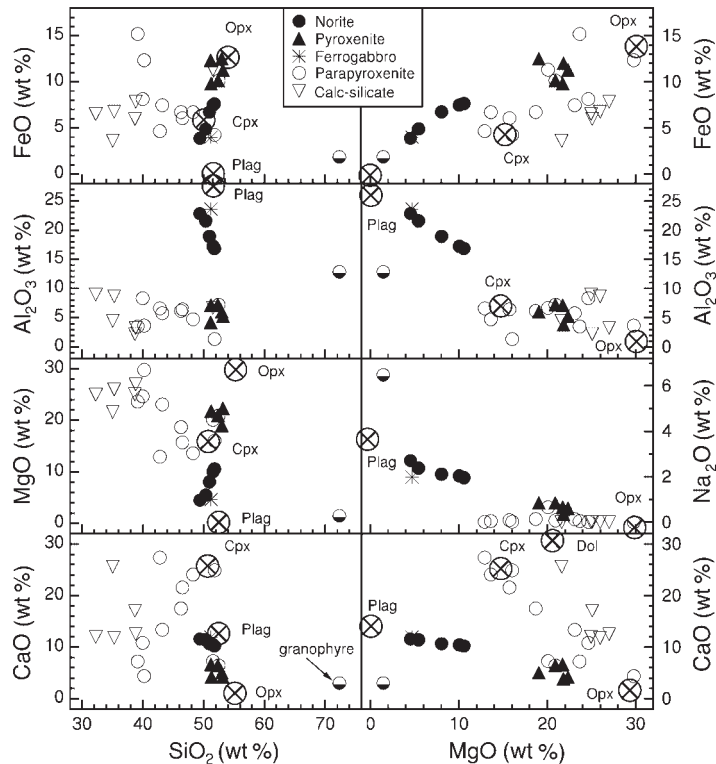


Fig. 4. Plot of various oxides vs SiO_2 and MgO for samples from and adjacent to the Platreef at Sandsloot. It should be noted that data were not normalized before plotting. Typical compositions for plagioclase, orthopyroxene, clinopyroxene (this work) and dolomite (Deer *et al.*, 1992) are also plotted.

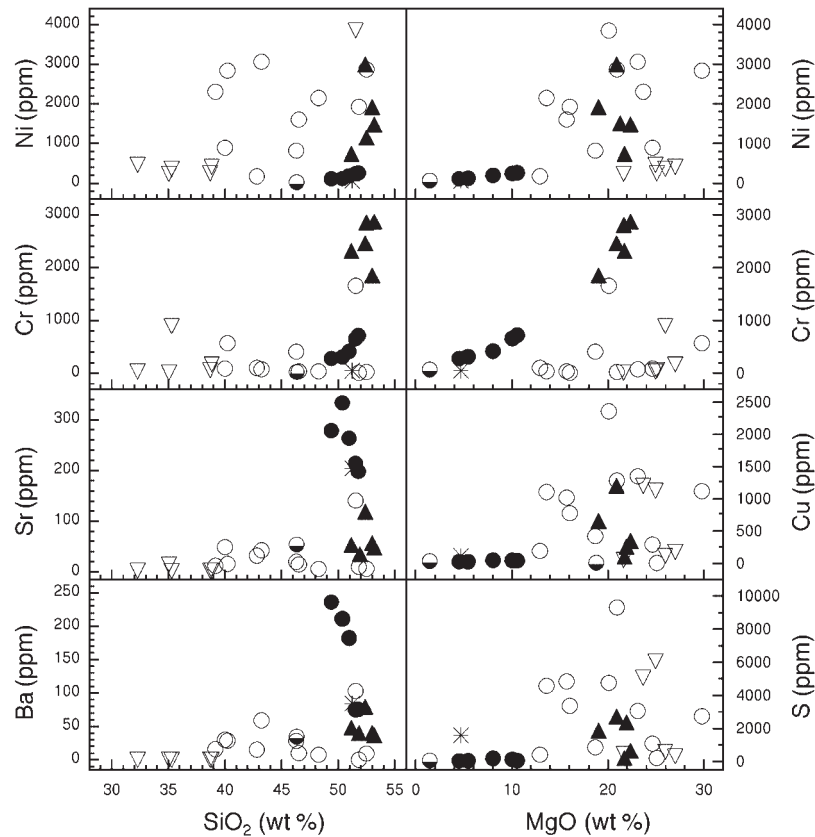


Fig. 5. Plot of various trace elements against SiO_2 and MgO for samples from and adjacent to the platreef at Sandsloot. Symbols as for Fig. 4.

calcsilicates, but both the parapyroxenites and calcsilicates have much higher Cu, Ni and S contents than the norites. The variation of Cu, Ni, Pb and Zn with S is shown in Fig. 6. In the norites and pyroxenites, Cu and Ni correlate positively with S, whereas Zn and Pb do not. In the parapyroxenites and calcsilicates there is no correlation between any of the elements and S. These data suggest that the high Ni and Cu content of the norites and pyroxenites is related to sulphide mineralization.

Variations in chemistry across the Platreef

The variation in selected oxides and trace elements with distance along the bench 20 traverse through the Platreef is shown in Fig. 7. The most obvious features of these traverses are abrupt changes in composition at the norite–pyroxenite boundary, and the transition from coherent variations in the norites and pyroxenites to much greater variability in the parapyroxenites. The norites have lower FeO and MgO but higher CaO than the pyroxenites, which is consistent with higher plagioclase and lower orthopyroxene in the norites. In the parapyroxenites, the CaO content increases and the MgO and Cr content

decreases with increasing distance away from the contact with the pyroxenites. This is consistent with a general decrease in the magmatic component of the mechanical mixture forming the parapyroxenites with distance away from the contact with the pyroxenites. The loss on ignition (LOI) is generally low (<3 wt %) in the magmatic rocks but is highest in the parapyroxenites closest to the contact with the pyroxenites. The high LOI is due mainly to high water content because these rocks do not now contain high levels of carbonate (see Table 6, below).

Sulphur is generally higher in the pyroxenites than in the norites, with variable levels in the parapyroxenites (up to nearly 1 wt %). There appears to be a general enrichment of S at the boundary between the pyroxenites and the parapyroxenites (Fig. 7), and similar enrichments are seen in Cu and Ni.

The sudden change in texture and mineralogical and chemical composition at the pyroxenite–norite contact suggests that the pyroxenites and norites crystallized from two separate magmas. However, we found no field evidence such as veins of norite within the pyroxenite (or the converse) to support this view. The coarse grain size of the pyroxenite is consistent with it crystallizing

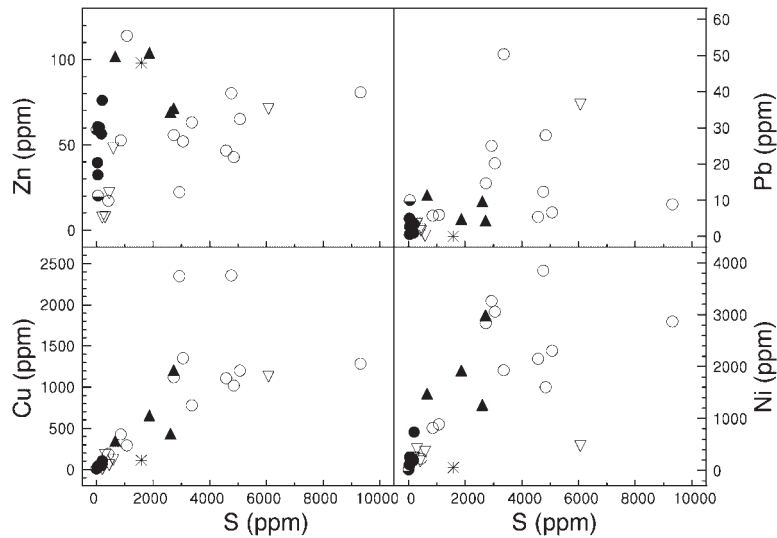


Fig. 6. Plot of Cu, Zn, Ni and Pb against S for samples from and adjacent to the Platreef at Sandsloot. Symbols as for Fig. 4.

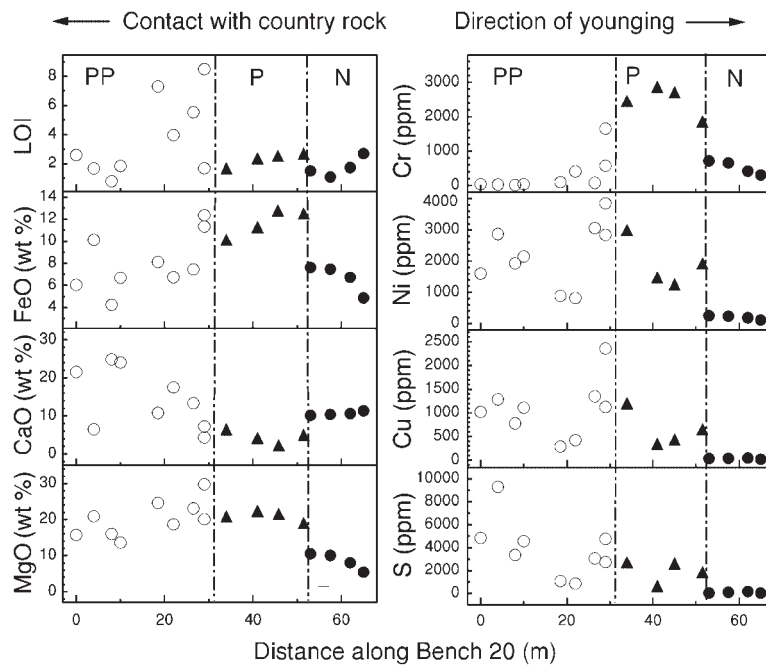


Fig. 7. Plot of various oxides and trace elements, and loss on ignition (LOI) vs distance along the bench 20 traverse through the Platreef. Distance is in metres where 0 m is close to the country rock and 65 m within the norites. The boundary between the norite (N) and the pyroxenite (P) is distinct chemically and in the field. The boundary between the pyroxenites and parapyroxenites (PP) is gradational.

before intrusion of the norites, as is the greater degree of visible alteration seen in the pyroxenites and the lack of dolomite xenoliths in the norites.

STABLE ISOTOPES

The Bellevue core

The $\delta^{18}\text{O}$ values of plagioclase and pyroxene samples from the Bellevue core are given in Table 3. Both

plagioclase and pyroxene show a restricted range in $\delta^{18}\text{O}$ values, from 7.0 to 8.3‰ (mean 7.9‰; $n = 18$) and 6.1–7.6‰ (mean 6.7‰; $n = 11$), respectively. The only exceptions are two samples that have plagioclase with much higher $\delta^{18}\text{O}$ values (10.4 and 13.1‰). Figure 8 shows the $\delta^{18}\text{O}$ value of plagioclase vs that of pyroxene for the Bellevue samples, and most form a tight cluster very close to the data obtained by Schiffries & Rye (1989) for Rustenburg Layered Suite rocks, including the

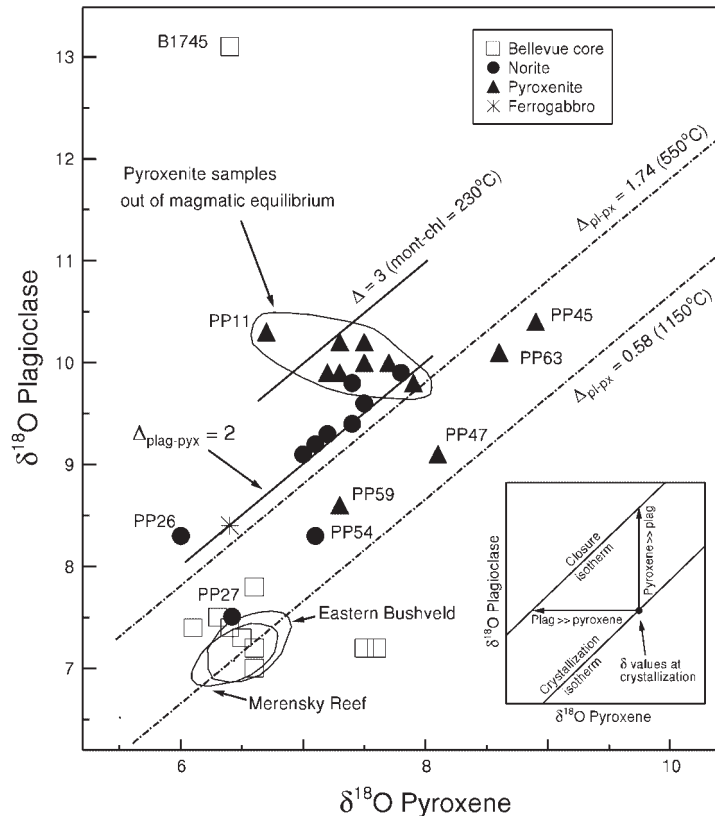


Fig. 8. Plot of the $\delta^{18}\text{O}$ value of plagioclase vs the $\delta^{18}\text{O}$ value of pyroxene for Bellevue and Platreef samples. Isotherms for 550 and 1150°C (corresponding to values of $\Delta_{\text{plagioclase-pyroxene}}$ of 1.74 and 0.58‰, respectively) are shown. These isotherms are based on the calibrations of Chiba *et al.* (1989) and assume a constant plagioclase composition of An_{60} . Most norites plot along the $\Delta_{\text{plagioclase-pyroxene}} = 2\text{‰}$ isotherm. Those pyroxenites that are not in magmatic O-isotope equilibrium are indicated. The montmorillonite–chlorite isotherm was calculated by combining the chlorite–water equation of Wenner & Taylor (1973) and the montmorillonite–water equation of Sheppard & Gilg (1996). The inset diagram shows the theoretical effects of slow cooling on bimineralic gabbro. Crystallization isotherm corresponds to difference in plagioclase and pyroxene $\delta^{18}\text{O}$ values and has a slope of one. Closure isotherm corresponds to difference in plagioclase and pyroxene $\delta^{18}\text{O}$ values at the temperature at which oxygen diffusion ceases. A rock dominated by plagioclase will migrate approximately horizontally across the diagram whereas a rock dominated by pyroxene will migrate vertically towards the closure isotherm. This follows from mass balance in that a large change in a small amount of pyroxene must be balanced by a small change in a large amount of plagioclase and vice versa.

Merensky Reef, from the eastern Bushveld. Exceptions are one sample (B1745) with a very large $\Delta_{\text{plagioclase-pyroxene}}$ and two samples with a slightly negative value of $\Delta_{\text{plagioclase-pyroxene}}$. These samples may have been affected by alteration.

The oxygen isotope stratigraphy of the Bellevue core is shown in Fig. 9, with data for the eastern Bushveld (Schiffries & Rye, 1989) also plotted, using the Main Zone–Upper Zone boundary as a reference. The two sets of data correspond well. The pyroxene $\delta^{18}\text{O}$ values in the Bellevue core decrease slightly with increasing stratigraphic height and $\Delta_{\text{plagioclase-pyroxene}}$ increases with height. The increase in $\Delta_{\text{plagioclase-pyroxene}}$ with increasing stratigraphic height is also seen in the data of Schiffries & Rye (1989) through a much larger stratigraphic thickness of the eastern limb of the Bushveld. The value of $\Delta_{\text{plagioclase-pyroxene}}$ would be expected to increase with stratigraphic height for two reasons: (1) in the Bellevue

core, the plagioclase becomes more sodic with height (Ashwal & Hart, 1995; Table 3) and $\Delta_{\text{plagioclase-pyroxene}}$ increases with decreasing anorthite content in the plagioclase (Chiba *et al.*, 1989); (2) decreasing crystallization temperature would have resulted in an increase in $\Delta_{\text{plagioclase-pyroxene}}$ with stratigraphic height.

A combination of both of the above effects would result in an increase in $\Delta_{\text{plagioclase-pyroxene}}$ [calculated from data of Chiba *et al.* (1989)] from 0.50‰ (An_{76} at 1150°C) to 0.75‰ (An_{47} at 1050°C). An additional effect, which is probably more important than (2), is that of closure to oxygen diffusion (e.g. Gilletti, 1986) where oxygen continues to equilibrate between minerals after crystallization to a temperature of $\sim 550^\circ\text{C}$. The final $\delta^{18}\text{O}$ values of minerals in the rock depend on modal mineralogy. Gabbros that contain mainly plagioclase (such as these) can show shifts in pyroxene $\delta^{18}\text{O}$ value of up to 1.16‰. This would account for the slight decrease in

Table 3: Oxygen isotope data for Bellevue core samples

Sample	Depth (m)	Type	$\delta^{18}\text{O}$ plag	$\delta^{18}\text{O}$ pyrox	% An
<i>Upper Zone</i>					
B352	352	Mottled anorthosite	7.6		47
B417	417	Anorthosite	7.4	6.1	
B612	612	Magnetite anorthosite	7.8		
B894	894	Magnetite leucogabbro	8.0		
B969	969	Anorthosite	8.3		
B1046	1046	Anorthosite	7.5		
B1146	1146	Magnetite leucogabbro	7.6		
B1318	1318	Magnetite leucogabbro	7.5	6.3	56
B1402	1402	Magnetite gabbro	7.8		
B1510	1510	Mottled anorthosite	7.2	6.6	57
B1560	1560	Magnetite gabbro	10.4		
<i>Main Zone</i>					
B1618	1618	Gabbro	7.3	6.5	59
B1745	1745	Gabbro	13.1	6.4	61
B1975	1975	Mottled anorthosite	7.0	6.6	64
B2115	2115	Mottled anorthosite	7.2	7.6	66
B2307	2307	Leucogabbro	7.4	6.4	70
B2446	2446	Leucogabbro	7.2	6.6	72
B2516	2516	Mottled anorthosite	7.8	6.6	74
B2703	2703	Anorthosite	7.1		
B2901	2901	Troctolite layer + opx	7.2	7.5	76

Plagioclase composition data from Ashwal & Hart (1995). Geology of core from Knoper & von Grunewaldt (1992). Complete core log is available at <http://users.iafrica.com/k/kn/knoper/faf1bic1.htm>. Depth is in metres measured along the core. The dip of the magmatic layering in the area of the borehole varies from 10 to 20°.

pyroxene $\delta^{18}\text{O}$ value with stratigraphic height shown in the Bellevue core. The most important conclusion from the above discussion is that the $\delta^{18}\text{O}$ value of the magma did not change significantly during crystallization of the Main and Upper Zones of the northern limb.

Platreef oxygen

Unlike the samples from the Bellevue core, the Platreef samples show considerable variation in plagioclase and pyroxene $\delta^{18}\text{O}$ values (see Table 4). The two most important features of Fig. 8 to note are that (1) plagioclase and pyroxene in the Platreef have generally higher $\delta^{18}\text{O}$ values than those of the Bellevue core, and (2) there are a significant number of samples with plagioclase and pyroxene that are not in oxygen isotope equilibrium at magmatic temperatures. The latter feature is generally considered to indicate water–rock interaction (e.g. Gregory & Criss, 1986) whereas the former is usually ascribed to crustal contamination (e.g. Taylor, 1980; James, 1981).

However, before any reliable conclusions can be reached concerning the extent of crustal contamination, the effects of post-magmatic alteration must be taken into account.

Most of the norites (and the ferrogabbro sample) plot slightly above the 550°C isotherm with average $\Delta_{\text{plagioclase-pyroxene}}$ values of $\sim 2.0\%$. By comparison, the Bellevue core samples have smaller values of $\Delta_{\text{plagioclase-pyroxene}}$ (0.6%) as does sample PP27, a norite collected from the Main Zone midway between Sandsloot and Potgietersrus (Fig. 1). One Platreef norite (PP54) has significantly lower $\Delta_{\text{plagioclase-pyroxene}}$ than the others. The pyroxene samples can be divided into two groups; those that plot within the 550 and 1150°C isotherms and appear to be in oxygen isotope equilibrium at magmatic temperatures, and those samples where $\Delta_{\text{plagioclase-pyroxene}}$ indicates disequilibrium. The latter group appears to form an array that shows a negative correlation between plagioclase and pyroxene $\delta^{18}\text{O}$ values. The implications for these data for sub-solidus fluid–rock interaction will be discussed below.

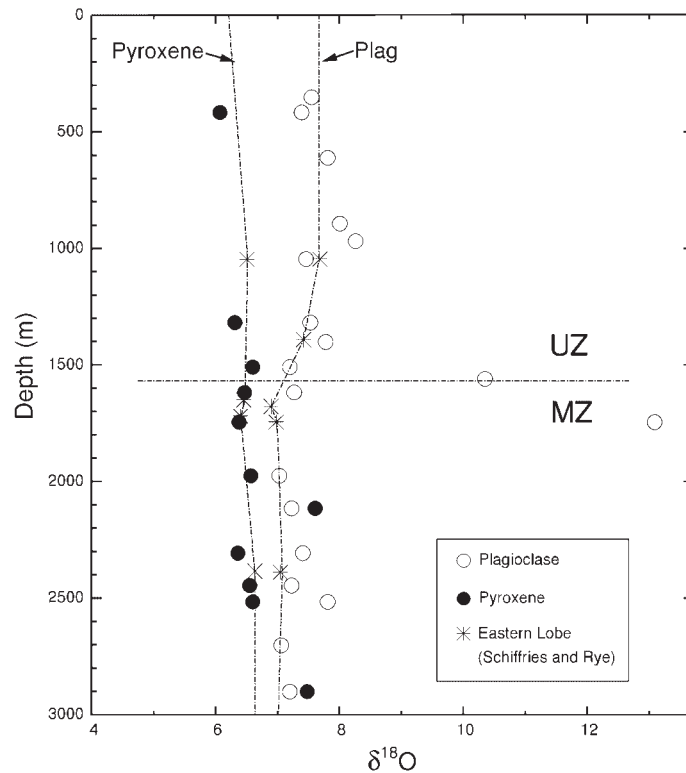


Fig. 9. Variation of plagioclase and pyroxene $\delta^{18}\text{O}$ values with depth in the Bellevue core through the northern limb. The boundary between the main (MZ) and upper (UZ) zones is indicated and the $\delta^{18}\text{O}$ values obtained for pyroxene and plagioclase from the eastern Bushveld (Schiffries & Rye, 1989) are plotted taking the UZ–MZ contact as a reference. The depth is that measured along the core. The dip of the igneous layering in this area varies from 10 to 20°. The maximum discrepancy between these data and the stratigraphic height data reported by Schiffries & Rye is 55 m (assuming a dip in the Bellevue core of 20°). It should be noted that the two lines join plagioclase and pyroxene data, respectively, from Schiffries & Rye (1989).

The $\delta^{18}\text{O}$ values of plagioclase and pyroxene show no systematic variation with major element oxides such as CaO, SiO₂ and MgO (Fig. 10). By contrast, whole-rock $\delta^{18}\text{O}$ values of the parapyroxenites (which contain no magmatic pyroxene and/or plagioclase) show a crude positive correlation with SiO₂ and CaO, and a negative correlation with MgO and LOI. Petrographic examination of the samples shows that those with low $\delta^{18}\text{O}$ values are rich in serpentine, and those with high $\delta^{18}\text{O}$ values are rich in diopside, and this is consistent with the $\delta^{18}\text{O}$ –oxide correlations. A possible interpretation is that diopside was relatively resistant to fluid–rock interaction whereas forsterite was not, being transformed to serpentine with significantly lower $\delta^{18}\text{O}$ value.

The variation in $\delta^{18}\text{O}$ value in the bench 20 and bench 14 traverse across the Platreef is shown in Fig. 11. In the bench 14 traverse, plagioclase and pyroxene show a slight increase towards the pyroxenite–parapyroxenite boundary, with diopside in the parapyroxenite being ~2.5‰ higher than in the pyroxenites. In the bench 20 traverse, where a greater thickness of parapyroxenite was sampled, the parapyroxenites increase in $\delta^{18}\text{O}$ value away

from the contact with the pyroxenite. Another feature of the bench 20 traverse is that $\Delta_{\text{plagioclase-pyroxene}}$ in the pyroxenites increases towards the contact with the parapyroxenites.

Two quartz–granophyre veins that intersect the bench 20 traverse (Fig. 2) have quartz $\delta^{18}\text{O}$ values of 10.1 and 12.2‰, whereas quartz in the calcite-bearing quartz–granophyre vein that cuts the pyroxenite has a $\delta^{18}\text{O}$ value of 6.9‰. As these veins are likely to be related to fluid–rock interaction, their $\delta^{18}\text{O}$ values are important for reconstructing the oxygen isotope composition of the alteration fluid.

Platreef hydrogen

Hydrogen isotope ratios were determined for biotite from six samples where the mineral appears to be a primary magmatic mineral. The Platreef rocks also contain a variety of secondary hydrous minerals and whole-rock dD values were determined on 11 other samples. These data are reported in Table 5, along with the water

Table 4: Oxygen isotope data for the Platreef and associated samples from Sandsloot Mine

Sample	Rock type	Distance (m)	$\delta^{18}\text{O}$ plagioclase	$\delta^{18}\text{O}$ pyroxene	$\delta^{18}\text{O}$ whole rock	$\delta^{18}\text{O}$ quartz
PP1	norite	65	9.6	7.5		
PP2	norite	62	9.9	7.8		
PP3	norite	57	9.4	7.4		
PP4	vein	56				12.2
PP5	norite	53	9.8	7.4		
PP6	vein	52				10.1
PP7	pyroxenite	51	9.9	7.2		
PP8	pyroxenite	45	9.8	7.9		
PP9	pyroxenite	41	9.9	7.3		
PP10	vein	34				10.3
PP11	pyroxenite	34	10.3	6.7		
PP12	pyroxenite	29	10.2	7.5		
PP13	parapyroxenite	29			6.6	
PP14	parapyroxenite	26			9.0	
PP15	parapyroxenite	22			8.0	
PP16	parapyroxenite	18			7.7	
PP17	parapyroxenite	10			9.4	
PP18	parapyroxenite	8			13.0	
PP19	parapyroxenite	4			10.1	
PP20	parapyroxenite	0			12.2	
PP24	ferrogabbro		8.4	6.4		
PP26	leconorite		8.3	6.0		
PP27	norite		7.4	6.8		
PP45	pyroxenite		10.4	8.9		
PP47	pyroxenite		9.1	8.1		
PP48	pyroxenite			7.5		
PP49	parapyroxenite				9.2	
PP54	norite	68	8.3	7.1		
PP55	norite	63	9.2	7.1		
PP56	norite	56	9.1	7.0		
PP57	norite	53	9.3	7.2		
PP58	pyroxenite	47		8.0		
PP59	pyroxenite	37	8.6	7.3		
PP60	pyroxenite	32	10.0	7.5		
PP61	pyroxenite	24	10.0	7.7		
PP62	pyroxenite	20	10.2	7.3		
PP63	pyroxenite	18	10.1	8.6		
PP64	parapyroxenite	11		11.3		
PP65	parapyroxenite	0		11.3		
PP67	Archaean granite			8.3		

PP27 collected at roadside 8 km NW Potgietersrus; PP67 from Archaean granite closest to Sandsloot.

content and a list of the hydrous minerals present. The biotite δD values vary from -60% in a norite sample (PP30) to -88% in a pyroxenite sample (PP 60). The

high water content of biotite in PP30 (5.58 wt %) indicates that it is altered to more water-rich minerals such as chlorite. The whole-rock δD values show a similar range

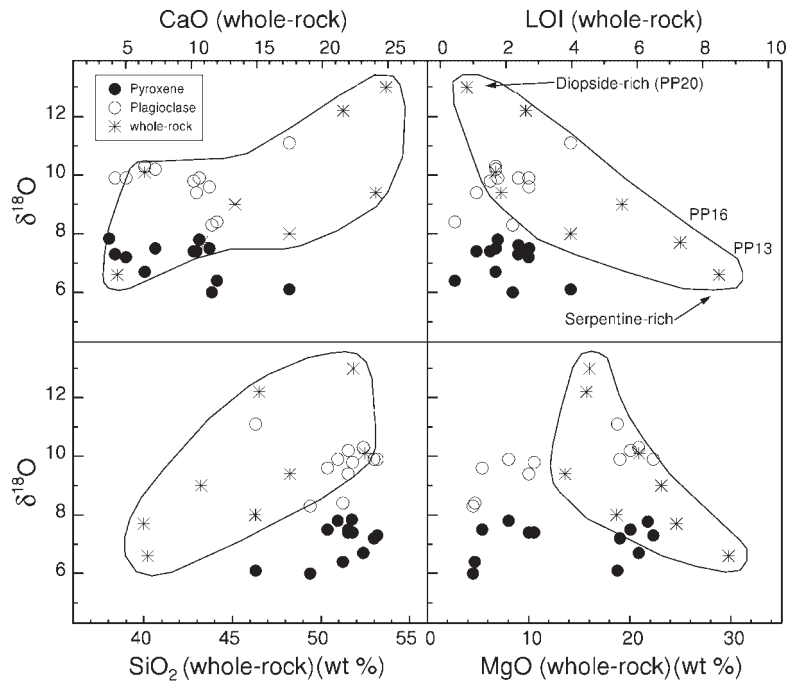


Fig. 10. Plot of $\delta^{18}\text{O}$ value of minerals and whole-rock samples from the Platreef vs oxide content and LOI of whole rock.

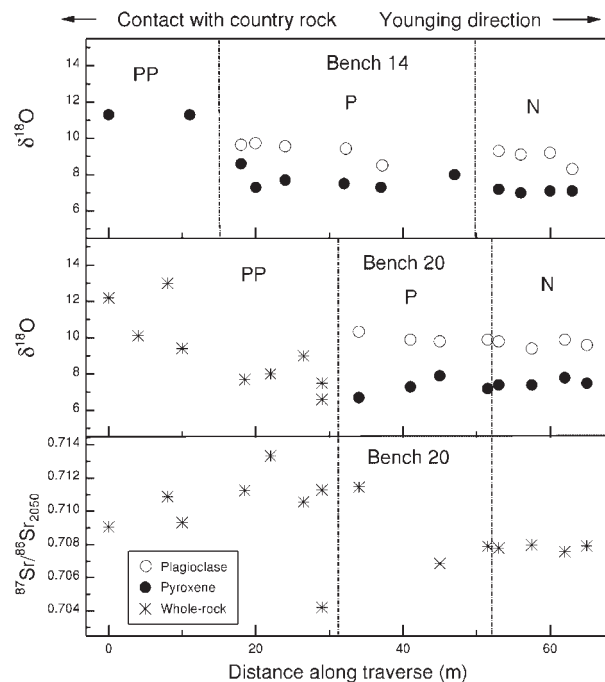


Fig. 11. Plot of $\delta^{18}\text{O}$ value vs distance from contact with calcilicite rocks for traverses along the bench 20 and bench 14 traverses, and initial Sr-isotope ratio vs distance along the bench 20 traverse.

to those of the biotites, from -64 to -99% . Figure 12 shows that the δD values of biotite and whole rock from

the Platreef show a vague positive correlation with H_2O^+ , an effect that is generally ascribed to magma degassing (e.g. Taylor, 1986). There is no correlation between biotite and whole-rock δD values and $\Delta_{\text{plagioclase-pyroxene}}$. The latter gives a crude indication of the amount of alteration given that plagioclase is more susceptible to alteration than pyroxene (e.g. Taylor, 1968). There is no correlation between hydrogen isotope data and major or trace element content.

The δD values of the biotite and the whole-rock samples overlap considerably, which is consistent with formation of biotite and other hydrous minerals during the same fluid-rock interaction. Although the hydrous minerals must have formed over a range of temperatures (biotite close to 700°C , chlorite close to 300°C), the mineral-water fractionation factor for hydrogen of biotite at 700°C is similar to that of chlorite at 300°C ($\Delta_{\text{mineral-water}} -30\%$, O'Neil, 1986). If fluid δD values are calculated from the biotite and whole-rock data using the same per mil fractionation (-30%), values similar to typical 'primary magmatic water' (that is, water that had equilibrated with the magma regardless of the origin of the water that was transported with the magma from its deep-seated source; Sheppard, 1986) are obtained (Fig. 12). Mathez *et al.* (1994), obtained very similar results for the Merensky Reef and related rocks in the Atok mine in the eastern limb of the Bushveld (Fig. 12). Schiffries & Rye (1990) obtained dD values between -34 and -71% for quartz vein inclusion water from the eastern

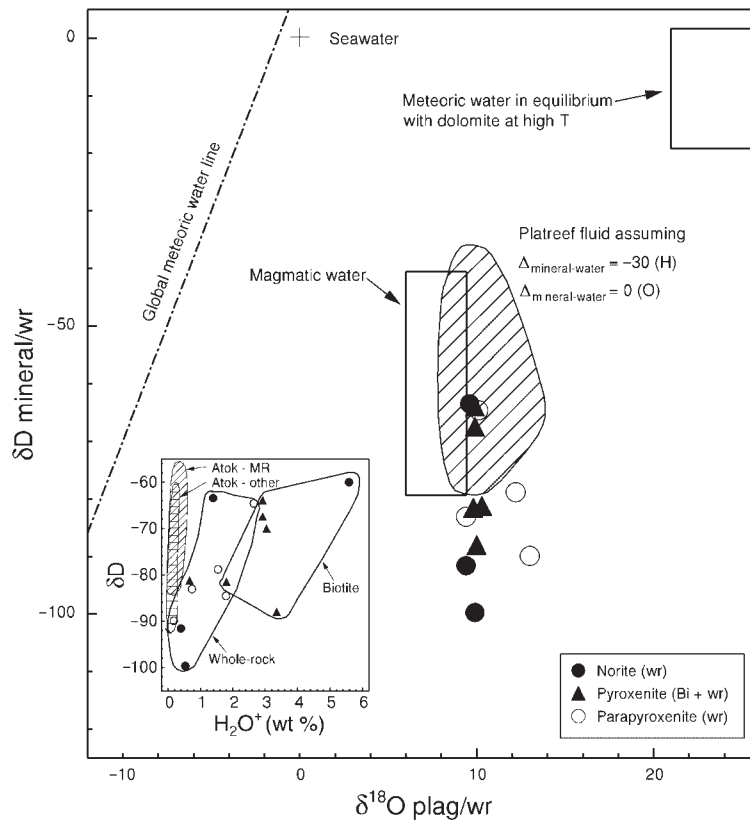


Fig. 12. Plot of δD of biotite or whole-rock (wr) vs $\delta^{18}O$ of plagioclase or whole rock. The range of values expected for typical magmatic water is from Taylor (1977). The inset diagram shows the variation of δD with H_2O^+ . The Atok-MR (Merensky Reef) and other Atok data are from Mathez *et al.* (1994). Global meteoric water line from Craig (1961).

lobe, which are also similar to the data obtained for the Platreef (allowing for mineral-water fractionations of the order of -30‰).

Carbonates

Carbonate minerals, calcite and dolomite, are present in small amounts in many of the Platreef rocks. The $\delta^{13}C$ and $\delta^{18}O$ values of the total carbonate present in a variety of whole-rock samples are given in Table 6. Both the $\delta^{13}C$ and $\delta^{18}O$ values show a very wide variation (Fig. 13). The majority of samples analysed have $\delta^{13}C$ values between 0 and -5‰ and $\delta^{18}O$ values $<15\text{‰}$. Three calcsilicates have relatively higher $\delta^{18}O$ values but lower $\delta^{13}C$ values. One parapyroxenite sample has a low $\delta^{18}O$ and $\delta^{13}C$ value. None of the Platreef samples contain carbonate with an isotope composition at all similar to unaltered dolomite in the area (Fig. 13).

Decarbonation during metamorphism causes changes in both $\delta^{13}C$ and $\delta^{18}O$ value in the remaining rock (e.g. Valley, 1986), and two Rayleigh decarbonation paths (using different fractionation factors) are shown in Fig.

13, starting from an arbitrary value appropriate for unaltered limestone. The samples with high $\delta^{18}O$ values ($>18\text{‰}$) and low $\delta^{13}C$ values are consistent with formation during closed-system decarbonation. By contrast, those samples with low $\delta^{18}O$ could not have formed during closed-system decarbonation. In the case of the parapyroxenites, the lowering of carbonate $\delta^{18}O$ values could have occurred during diffusional equilibration with the igneous silicate rocks. Low $\delta^{18}O$ values in the calcsilicate carbonates must, however, reflect interaction with an externally derived fluid. The carbonate in the norite and in the vein represent reprecipitated carbonate derived from relatively undecarbonated country rock. Graphite nodules, a few centimetres in diameter, from the calcsilicate rocks have an average $\delta^{13}C$ value of -26.9‰ (Table 6), which is considerably more negative than the $\delta^{13}C$ values of the host calcsilicate rocks (average -4.9‰ , $n = 13$). The $\delta^{13}C$ value of the graphite presumably reflects the original sedimentary value and indicates a lack of equilibration of carbon isotopes between graphite and carbonate during metamorphism because $\Delta_{\text{calcite-graphite}}$ is $<6\text{‰}$ above 500°C (Chacko *et al.*, 1991).

Table 5: Hydrogen isotope data for Platreef and associated rocks from Sandsloot Mine

Sample	Rock type	Hydrous minerals	δD bi	δD wr	H ₂ O ⁺
PP1	norite	ser, chl, bi		-64	1.39
PP2	norite	ser, chl, bi		-99	0.53
PP3	norite	ser, chl, bi		-92	0.40
PP7	pyroxenite	bi, chl, amp, ser	-68		2.92
PP8	pyroxenite	bi, chl, amp, ser	-82		1.80
PP9	pyroxenite	bi, chl, amp, ser	-64		2.92
PP11	pyroxenite	bi, chl, amp, ser		-81	0.66
PP17	parapyroxenite	bi, chl		-83	0.74
PP18	parapyroxenite	bi, chl		-90	0.18
PP19	parapyroxenite	bi, chl		-65	2.65
PP20	parapyroxenite	bi, chl		-79	1.54
PP22	calcsilicate	serp, chl		-89	—
PP30	norite	bi, chl, amp, ser	-60		5.58
PP33	parapyroxenite	bi		-85	1.79
PP43	pyroxenite	bi, chl, amp, ser	-70		3.04
PP60	pyroxenite	bi, chl, amp, ser	-88		3.35

Present-day spring water in the mine has a δD of -22‰ and $\delta^{18}O$ of -3.78‰ (this work).

STRONTIUM ISOTOPES

Strontium isotope data for samples from the bench 20 traverse at Sandsloot are reported in Table 7. Measured $^{87}Sr/^{86}Sr$ ratios of both the norites and pyroxenites, and the parapyroxenites show a good correlation with Rb/Sr (Fig. 14) and the line of best fit has a gradient close to the accepted age of intrusion (2050 Ma, Walraven *et al.*, 1990). Taken as a whole, the data indicate an average initial ratio of 0.7093, which is higher than the generally accepted values for the Main Zone of the Bushveld intrusion elsewhere (0.7075–0.7090; Hamilton, 1977; Harmer & Sharpe, 1985). However, six of the seven norite and pyroxenite samples form an array with a line of best fit approximately parallel to the 2050 Ma reference line but with lower initial ratio (0.7080), and eight out of nine of the parapyroxenite and calcsilicate samples form an array with similar apparent 'age' but with a higher initial ratio (0.7100).

Initial Sr-isotope ratios (at 2050 Ma) are plotted against distance across the Platreef in Fig. 11 and it is evident that the non-magmatic rocks generally have significantly higher initial Sr-isotope ratios, and that there is a sharp change in initial Sr-isotope ratio, except for samples taken very close to the contact. The similarity in apparent 'age' between the magmatic and country rocks indicates that the Sr-isotope ratios of the latter were reset at the time of intrusion, but the low Sr concentration and higher initial ratio of the immediate country rocks suggest that

diffusion of Sr from the magmatic rocks into the footwall of the Platreef was limited.

The correlation between initial Sr-isotope ratio and MgO, CaO and SiO₂ is poor (as expected given the rocks are cumulates) (Fig. 15), but in general samples with high MgO and CaO, and low SiO₂ have higher initial Sr-isotope ratios. There is no apparent correlation between $\delta^{18}O$ and initial Sr-isotope ratio (Fig. 15), but this is understandable given the low Sr content of the non-magmatic potential contaminants.

OXYGEN ISOTOPE COMPOSITION OF THE PARENT MAGMA

The norites and pyroxenites of the Platreef and the rocks of the Bellevue core do not represent quenched liquid compositions. It is, therefore, necessary to estimate the magma $\delta^{18}O$ value from mineral data using appropriate fractionation factors and assumptions about cooling history. It was shown above (Fig. 8) that most of the Bellevue core samples, and some Platreef pyroxenite samples, have plagioclase and pyroxene $\delta^{18}O$ values that are consistent with oxygen isotope equilibrium at magmatic temperatures. Samples that plot significantly outside the closure and crystallization isotherms (Fig. 8) have probably been affected by alteration, and the nature of this process is discussed below. Pyroxene is less susceptible to exchange with fluids than is plagioclase (e.g. Gregory

Table 6: Carbon and oxygen isotope data for calcite and graphite at the Platreef at Sandsloot Mine

Sample	Rock type	% carb	$\delta^{18}\text{O}$	$\delta^{13}\text{C}$
Carbonates				
<i>Platreef</i>				
PP10	qtz-calcite vein	3.6	6.9	-2.3
PP15	parapyroxenite	0.2	7.3	-9.8
PP31	calcsilicate	1.2	19.4	-7.9
PP32	calcsilicate	0.2	19.1	-12.9
PP33	calcsilicate	3.5	13.0	-2.4
PP34	parapyroxenite	1.0	14.0	-4.2
PP36	calcsilicate	4.1	25.5	-7.6
PP41	calcsilicate	0.7	14.9	-0.4
PP49	calcsilicate	0.9	12.8	-2.3
PP53	calcsilicate	0.9	15.4	-3.7
PP57	norite	2.1	11.2	-2.7
PP64	parapyroxenite	0.3	12.3	-4.3
PP65	calcsilicate	0.5	12.1	-3.8
<i>Malmani dolomite</i>				
CA1	Makapansgat Valley	27.6	21.1	-2.2
CA2	Makapansgat Valley	29.2	22.0	-2.6
CA3	Makapansgat Valley	87.8	23.1	-1.7
WB1	Nr Wolkberg Cave	100.0	23.2	-0.8
Graphite				
PP39	calcsilicate			-27.3
PP52	calcsilicate			-26.6

All samples reacted at 50°C; $\alpha_{\text{CO}_2\text{-carb}}$ assumed to be 1.009 (calcite). The effect of using the calcite-CO₂ fractionation factor for pure dolomite is to overestimate $\delta^{18}\text{O}$ by ~1.6‰, thus the total carbonate $\delta^{18}\text{O}$ values may be slightly too high if the sample also contains dolomite (see text). Malmani dolomite samples from east of Potgietersrus (Makapansgat Valley and Wolkberg cave; both >10 km from contact with intrusion).

& Taylor, 1981), and the pyroxene $\delta^{18}\text{O}$ values should, therefore, provide the best indication of changes in the magma $\delta^{18}\text{O}$ value. Changes in pyroxene $\delta^{18}\text{O}$ value resulting from slow cooling between the temperatures of crystallization and closure to oxygen diffusion are dependent on factors such as mineral mode, grain size and cooling rate (see inset to Fig. 9).

The shift in pyroxene $\delta^{18}\text{O}$ value caused by closure effects during slow cooling is comparatively small in magnitude, but is difficult to quantify because the rate of cooling is not known. The pyroxene $\delta^{18}\text{O}$ values will decrease during slow cooling because $\Delta_{\text{feldspar-pyroxene}}$ becomes larger with decreasing temperature. Let us consider the case of a biminerallitic gabbro with 50% plagioclase

and 50% pyroxene. At the moment of crystallization from a mantle-derived basaltic magma with a $\delta^{18}\text{O}$ value of 5.7‰, this rock will have plagioclase with a $\delta^{18}\text{O}$ value of 5.90‰, pyroxene with a $\delta^{18}\text{O}$ value of 5.40‰, and a whole-rock $\delta^{18}\text{O}$ value of 5.65‰, assuming $\Delta_{\text{plagioclase-pyroxene}} = 0.5$, appropriate for plagioclase (An₇₀) and pyroxene at 1150°C (Chiba *et al.*, 1989) and that $\Delta_{\text{plagioclase-melt}} = +0.2$ ‰ (Kyser *et al.*, 1981). If cooled slowly to ~750°C, a plausible closure temperature for pyroxene in a medium-grained igneous rock, $\Delta_{\text{plagioclase-pyroxene}} = 1$ ‰ (Chiba *et al.*, 1989) and the $\delta^{18}\text{O}$ values of the coexisting plagioclase and pyroxene will therefore be 6.15 and 5.15‰, respectively. It should be noted that the magnitude of the change in pyroxene $\delta^{18}\text{O}$ value is the same as that of plagioclase because its modal abundance is the same. Thus the pyroxene $\delta^{18}\text{O}$ value is now 0.55‰ less than the $\delta^{18}\text{O}$ value of the original magma as opposed to the original $\Delta_{\text{melt-pyroxene}}$ value of -0.3‰. For these reasons we will assume that the original magmas that produced the Bellevue and Sandsloot cumulates had $\delta^{18}\text{O}$ values 0.55‰ higher than the measured $\delta^{18}\text{O}$ values of the pyroxene

The majority of the Bellevue samples have pyroxene $\delta^{18}\text{O}$ values between 6.1 and 6.6‰ (mean 6.4‰, $n = 9$). These data indicate that the original magma had a $\delta^{18}\text{O}$ value of ~7.0‰, similar to the estimate of Schiffries & Rye (1989) for the eastern limb of the Bushveld. The highest $\delta^{18}\text{O}$ value obtained for pyroxene from the Platreef was for pyroxenite sample PP45, which has pyroxene and plagioclase in apparent oxygen isotope equilibrium at magmatic temperatures (Fig. 9). The pyroxene $\delta^{18}\text{O}$ value of 8.9‰ indicates crystallization from a magma having a $\delta^{18}\text{O}$ value of 9.5‰. These values indicate that the Platreef magmatic rocks formed from magma(s) that were significantly more contaminated than is generally the case for the Bushveld.

CRUSTAL CONTAMINATION

The oxygen isotope constraints on the amount of crustal contamination in the eastern limb of the Bushveld and in the Merensky Reef have been discussed in detail by Schiffries & Rye (1989) and Reid *et al.* (1993), respectively. As discussed above, the Bellevue samples have very similar oxygen isotope compositions to the rest of the Bushveld complex. The magma(s) from which these rocks crystallized had a $\delta^{18}\text{O}$ value estimated to be 7.0‰, which is significantly higher than expected from an uncontaminated mantle-derived magma (5.7‰, Ito *et al.*, 1987). Schiffries & Rye (1989) suggested that partial melting of an ¹⁸O-enriched mantle was an unlikely explanation for the high $\delta^{18}\text{O}$ values in the Bushveld magmas. This explanation has become even less tenable since that time because mantle xenoliths from the

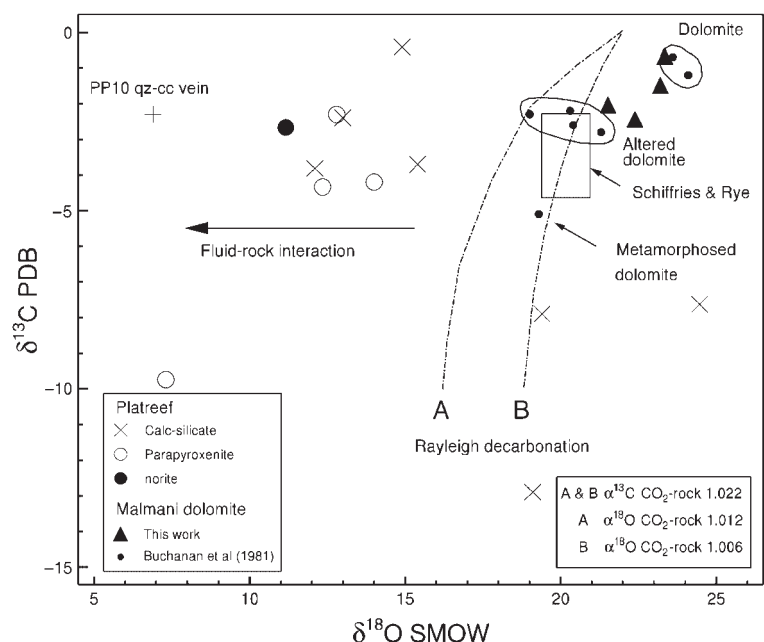


Fig. 13. Plot of $\delta^{13}\text{C}$ vs $\delta^{18}\text{O}$ of carbonate minerals in calcsilicate rocks, parapyroxenite rocks and in a sample of norite and PP10 (a quartz-granophyre vein). Also shown are the paths for calcite undergoing Rayleigh decarbonation, with the fractionation factors indicated (Valley, 1986). The theoretical decarbonation represents Rayleigh decarbonation starting from the composition of an arbitrary ‘unaltered’ carbonate and assumes that the fluid was pure CO_2 . If a mixed $\text{CO}_2\text{-H}_2\text{O}$ fluid was present, H_2CO_3 would be more likely to be the dominant carbon-bearing species, which has a smaller carbon isotope fractionation with calcite than CO_2 (e.g. Cartwright & Buick, 1999), and the effects would be less pronounced. The composition of dolomite, hydrothermally altered dolomite and metamorphosed dolomite from the vicinity of Sandsloot is also shown [data from Buchanan *et al.* (1981)], as are the field for dolomite data from Schiffries & Rye (1990) and Malmani dolomite analysed during this work (Table 6).

Kaapvaal craton show no evidence for elevated $\delta^{18}\text{O}$ values (Mattey *et al.*, 1994). The other important constraint is that the magma $\delta^{18}\text{O}$ values in the eastern, western or northern limb do not appear to have changed during crystallization. This suggests that the magmas became contaminated before emplacement and were well mixed at the time of intrusion (Schiffries & Rye, 1989).

Schiffries & Rye (1989) concluded that the rocks of the Transvaal Supergroup were the likely contaminants because of their availability and relatively high $\delta^{18}\text{O}$ values (9–15‰), and that simple mixing models indicate between 10 and 29% contamination. The available $\delta^{18}\text{O}$ values for Archaean granitic rocks of the Kaapvaal craton suggest typical values of around 6–8‰ (Taylor, 1968; Barker *et al.*, 1976; Faure & Harris, 1991), and Archaean granite 3 km from Sandsloot Mine (PP67, Table 4) has a whole-rock $\delta^{18}\text{O}$ value of 8.3‰. The oxygen isotope composition of lower crust in the region is not known. However, the average $\delta^{18}\text{O}$ value of lower-crustal rocks exposed in the Vredefort impact structure 100 km to the south (La Grange *et al.*, 2000) is 8.67‰ ($n = 35$). It would require 44% contamination by material having a $\delta^{18}\text{O}$ value of 8.67‰ to raise the $\delta^{18}\text{O}$ value of the Bushveld magma from 5.7 to 7.0‰, and greater degrees of contamination (49%) by the adjacent Archaean granite

(PP67). Amounts of contamination as high as this are unrealistic, and we therefore concur with Schiffries & Rye (1989) that the Transvaal Supergroup sedimentary rocks are the most viable contaminants. It should be emphasized that these estimates of amount of contamination are minimum values because they assume simple mixing, rather than assimilation accompanied by crystal fractionation (AFC, DePaolo, 1981). If the contamination process took place in a magma chamber at a lower level in the crust before emplacement, it could have been via an AFC process, in which case the integrated amount of contamination would have had to have been larger than for simple mixing.

Pyrroxenes in the pyroxenite rocks of the Platreef at Sandsloot have $\delta^{18}\text{O}$ values that are up to 2.4‰ higher than pyroxenes in the Bellevue norites. Although differences in grain size and mode might have slightly accentuated this difference (e.g. inset to Fig. 9), it is clear that the Platreef magmas were affected by greater degrees of contamination than the Bushveld in general. The country rock in the area is dolomite, and unaltered dolomite in the area typically has a $\delta^{18}\text{O}$ value of 19–24‰ (Buchanan *et al.*, 1981; Table 6). Dolomite is by far the most likely contaminant, not only because of its proximity and the presence of calcsilicate xenoliths, but also because

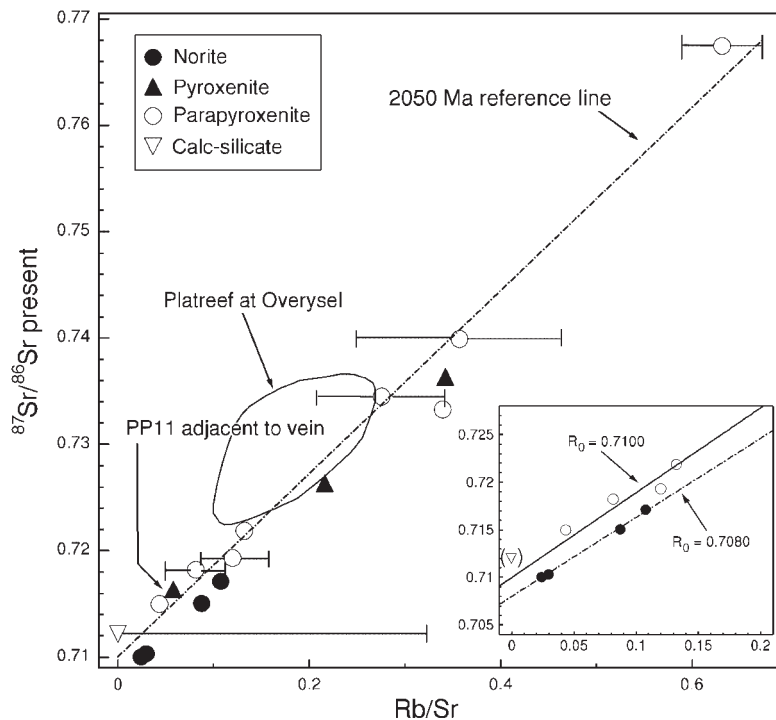


Fig. 14. Plot of $^{87}\text{Sr}/^{86}\text{Sr}$ vs Rb/Sr for Platreef samples. Large errors in the Rb/Sr ratio caused by low Sr concentration are indicated, as is the 2050 Ma reference line (starting from an arbitrary initial ratio of 0.710). The inset diagram shows the low Rb/Sr part of the diagram, emphasizing the different lines of best fit through the norite–pyroxenite and parapyroxenite–calc-silicate data (lines of best fit calculated for all the data, not just the data plotted in the inset diagram). The data field for Overysel, where the Platreef is in contact with Archaean granite, is from Cawthorn *et al.* (1985).

its high $\delta^{18}\text{O}$ value produces a much greater shift in $\delta^{18}\text{O}$ per unit assimilated than the other potential contaminants. The dolomite has very low Sr content and dolomite contamination would not, therefore, affect the Sr-isotope composition of the magma.

Because of the thermal, and possibly hydrothermal, effect of the intrusion on the dolomite, the nature of the contaminant could vary from unaltered dolomite through decarbonated dolomite to material with the same chemical and isotope composition as the calc-silicate material in the parapyroxenites. The calc-silicate material in the parapyroxenites has $\delta^{18}\text{O}$ values that are too low (<13‰) to be realistic contaminants but this may reflect ^{18}O depletion as a result of fluid–rock interaction and/or diffusional equilibration with the magmatic rocks during slow cooling. Dolomite that became decarbonated in the absence of significant volumes of external fluid might be expected to have $\delta^{18}\text{O}$ values only a few per mil lower than the unaltered dolomite (e.g. Valley, 1986, p. 453) and is, therefore a realistic contaminant in terms of its high $\delta^{18}\text{O}$ value. An alternative for contamination mechanism is that the magma absorbed appreciable quantities of ^{18}O -enriched CO_2 produced by decarbonation of the dolomite. Physical evidence for this

process in the form of primary CO_2 inclusions in minerals is, however, lacking.

Simple mixing calculations indicate that assimilation of 18% unaltered dolomite by the Bellevue norite magma would raise the magma $\delta^{18}\text{O}$ value by 2.4‰ (assuming that the magma contained 1.3 times the oxygen than the dolomite). The effect of dolomite contamination on the phase relations of the crystallizing magma is considered in a highly simplified manner with respect to the ternary diopside–forsterite–silica phase diagram (Fig. 16). The composition of the Platreef magma is poorly constrained but possible candidates are the B2 magma of Sharpe (1981) proposed as parental to the Critical Zone, or a more fractionated version of the parental magma proposed for the Lower Zone (Davies *et al.*, 1980). The only cumulus mineral observed in rocks of the Platreef is orthopyroxene, which suggests a parent liquid that plots in the liquid + enstatite field. Provided the material assimilated plots close to the diopside apex, with moderate amounts of contamination, the resultant composition will not plot outside [fractionated B2 magma, or Davies *et al.* (1980) magma] the liquid + enstatite field and rocks containing only cumulus orthopyroxene would still be the first to form. The dolomite in contact with the

Table 7: Rb–Sr isotope data for samples from the Platreef

Sample	Lithology	Rb (ppm)	Sr (ppm)	Rb/Sr	$^{87}\text{Rb}/^{86}\text{Sr}$	$^{87}\text{Sr}/^{86}\text{Sr}$	$^{87}\text{Sr}/^{86}\text{Sr}_i$
PP1	N	36	333	0.108	0.3111	0.71711(2)	0.70792
PP2	N	23	264	0.087	0.2526	0.71505(2)	0.70758
PP3	N	5.2	214	0.024	0.0702	0.71003(2)	0.70796
PP5	N	5.9	198	0.030	0.0861	0.71033(2)	0.70779
PP7	P	12	57	0.217	0.6284	0.72636(8)	0.70788
PP8	P	12	34	0.341	0.9892	0.73607(6)	0.70685
PP11	P	6.8	119	0.057	0.1658	0.71637(2)	0.71145
PP12	PP	6.1	141	0.043	0.1256	0.71499(2)	0.71128
PP13	PP	5.4	16	0.340	0.9844	0.73327(14)	0.70421
PP14	PP	5.6	42	0.132	0.3833	0.72188(2)	0.71057
PP15	PP	13	20	0.633	1.841	0.76756(5)	0.71332
PP16	PP	4.0	49	0.082	0.2368	0.71822(2)	0.71125
PP17	PP	2.1	5.8	0.362	1.050	0.73991(8)	0.70932
PP18	PP	2.7	9.7	0.278	0.8069	0.73449(5)	0.71088
PP20	PP	1.8	15	0.122	0.3520	0.71930(2)	0.70906
PP32	CS	0.0	2.1	—	—	<0.71220(3)	<0.71220

N, norite; P, pyroxenite; PP, parapyroxenite; CS, calc-silicate. Rb and Sr by XRF. 1σ errors on Rb are <0.7 ppm, errors on Sr are <1.2 ppm for samples with >50 ppm Sr and <0.7 ppm for samples with Sr <50 ppm. The figure in parentheses after the measured Sr-isotope ratio is the 2σ error based on counting statistics and applies to the last digit(s). Initial ratio calculated using an age of 2.05 Ga.

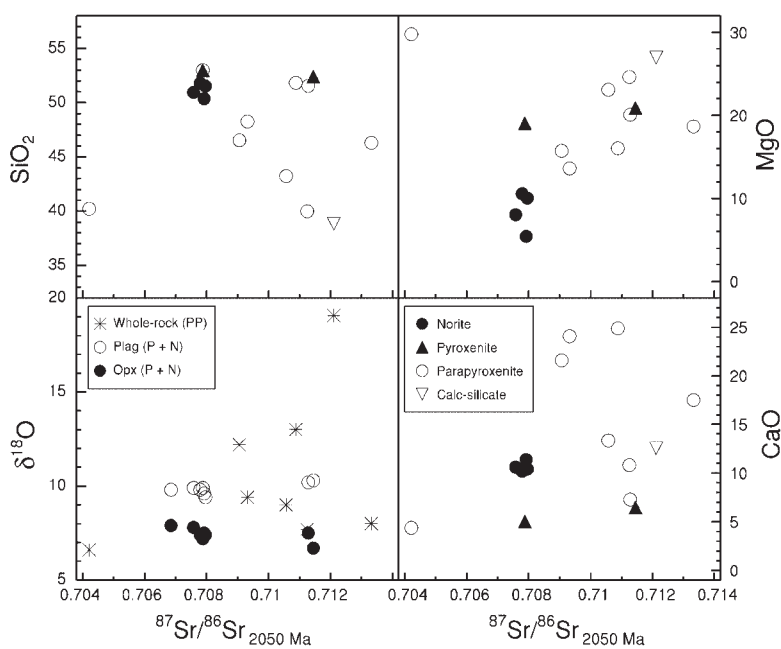


Fig. 15. Plot of $\delta^{18}\text{O}$ (minerals and whole rock), and whole-rock SiO_2 , MgO and CaO vs initial Sr-isotope ratio (whole rock).

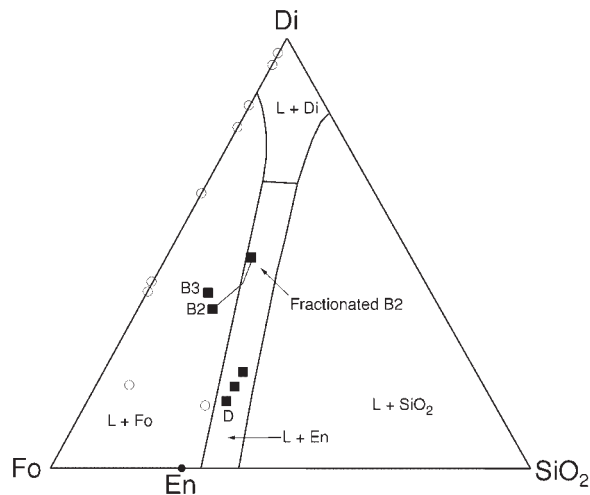


Fig. 16. Diopside (Di)–forsterite (Fo)–silica phase diagram showing position of liquid + forsterite, silica, diopside and enstatite at low pressure. ■, various parental magma compositions proposed for Bushveld. D, Davies *et al.* (1980), with additional points corresponding to 10 and 20% fractionation of enstatite. B2 and B3 are parental magmas to the critical and main zones, respectively (Sharpe, 1981). The fractional crystallization path for B2 is indicated.

Platreef at Sandsloot is from the Malmani subgroup. Unmetamorphosed Malmani rocks consist of chert-rich and chert-poor units, whereas metamorphosed carbonate rocks in the area are dominated by diopside with only minor forsterite (Nell, 1985). Dolomite assimilation is not, therefore, inconsistent with the observed cumulus mineralogy in the Platreef.

At Sandsloot, the norite with the lowest pyroxene $\delta^{18}\text{O}$ value (PP26) was collected from the west wall of the open pit (Fig. 2) and is not associated with the Platreef. It and the nearby ferrogabbro (PP24) have pyroxene $\delta^{18}\text{O}$ values that are within the range shown by the Bellevue samples. Norite sample PP2 has the pyroxene with the highest $\delta^{18}\text{O}$ value (7.8‰), which is 1.8‰ higher than PP26. This difference in pyroxene $\delta^{18}\text{O}$ value is consistent with ~13% contamination with dolomite. If, as discussed above, the norites crystallized from a second magma, which intruded the pyroxenites, the pyroxenites would have insulated the norite magma from direct contact with the dolomite. Thus the high $\delta^{18}\text{O}$ values of the norites adjacent to the pyroxenites could reflect either assimilation of already contaminated pyroxenites or mixing of norite magma with contaminated supernatant magma above the pyroxenite layer. Petrographic evidence for either process is, however, lacking.

Cawthorn *et al.* (1985) investigated the interaction of the Platreef with the country rock at Overysel, ~5 km north of Sandsloot, where the Platreef is in contact with Archaean granite. The initial Sr-isotope ratios of the Platreef magmatic rocks at Overysel are generally higher

than at Sandsloot (0.7079–0.7227, mean 0.7148). Cawthorn *et al.* (1985) pointed out that although the high initial Sr-isotope ratios in the Platreef could be explained by 60% contamination with Archaean granite, such high degrees of contamination are not supported by variations in the major elements. Cawthorn *et al.* (1985) therefore proposed that the contamination occurred via a partial melt or fluid phase derived from the granite. Cawthorn *et al.* (1985) rejected the possibility of contamination by dolomite because the $^{87}\text{Sr}/^{86}\text{Sr}$ ratios of the dolomite at 2050 Ma were not high enough to have produced the variation in initial Sr-isotope ratios in the Platreef at Overysel. At Sandsloot, contamination by dolomite is consistent with both the stable and radiogenic isotope data. The differences observed in the Platreef at these two locations thus seem to be a function of the nature of the immediate country rock.

FLUID–ROCK INTERACTION

The following lines of evidence suggest that the Platreef was affected by fluid–rock interaction to a much greater degree than is generally the case in the Bushveld and, specifically, in the Merensky Reef:

- (1) the per mil difference between plagioclase and pyroxene (2–3.6‰) in some of the pyroxenites is not consistent with formation at magmatic temperatures;
- (2) the per mil difference between plagioclase and pyroxene (~2‰) in the norites and the ferrogabbro in the hanging wall of the Platreef is higher than that observed in similar rock types at higher levels of the northern limb;
- (3) hydrous minerals are relatively abundant in the Platreef;
- (4) calcisilicate rocks within and just below the Platreef shown evidence for ^{18}O depletion, which must have occurred during interaction with fluids;
- (5) sulphide mineralization in the Platreef encompasses both the pyroxenites and the dominantly metacarbonate parapyroxenites, which suggests that the sulphides were, at least in part, transported by fluids.

Although these features could result from a number of different periods of fluid–rock interaction, the lack of disturbance to the Sr-isotope system suggests that the alteration event(s) took place soon after intrusion.

Origin of the fluid

At the time of intrusion, the Bushveld complex was situated at relatively low latitude (about 20°; Hattingh, 1983) and meteoric water at that time would not be expected to have been much different from present-day ground water. Water collected from a spring in the lowest part of the mine at Sandsloot (24°S and 500 km from

the Indian Ocean) has a δD value of -22‰ (Table 5). The δD values of biotites and whole rock, and $\delta^{18}\text{O}$ values of plagioclase and whole rock, have been used to reconstruct the isotope composition of the fluid that interacted with the Platreef (Fig. 12). The calculated composition of the Platreef fluids is typical of magmatic fluid (e.g. Taylor, 1977) and distinct from meteoric water and meteoric fluid in equilibrium with dolomite.

Although it cannot be proved, it seems likely that the quartz-granophyre veins that cut the Platreef were associated with the fluid–rock interaction. Given that these veins have granophyric margins, they must have formed at high temperatures ($>500^\circ\text{C}$) during slow cooling of Platreef and overlying norites. Quartz from the three veins that intersect the bench 20 traverse (Fig. 3) has (^{18}O values between 10.1 and 12.2‰. At relatively high temperatures, the mineral–water fractionation factors are low ($\Delta_{\text{quartz-water}}$ is $+3\text{‰}$ at 550°C , Clayton *et al.*, 1972), which means that fluid in equilibrium with the quartz would have had a $\delta^{18}\text{O}$ value of $\sim 7\text{--}9\text{‰}$). At temperatures between 500 and 700°C , $\Delta_{\text{calcite-water}}$ changes from $+2$ to 0‰ . At these temperatures, interaction between a magmatic fluid ($\delta^{18}\text{O} \sim 7\text{--}9\text{‰}$), and the dolomite would decrease the $\delta^{18}\text{O}$ value of the dolomite (or calcsilicate) towards the $\delta^{18}\text{O}$ value of the fluid. Low $\delta^{18}\text{O}$ values of carbonate in the calcsilicates ($\delta^{18}\text{O}$ as low as 12.2‰) are consistent with interaction with a magmatic fluid at high temperature. The ultimate origin of the fluid is uncertain; it is probable that the fluid is a mixture of water from the source region of the magma and water derived during the contamination process(es).

Hydrothermal interaction in gabbroic rocks normally produces steep arrays on a plagioclase vs pyroxene δ – δ diagram such as Fig. 8 (e.g. Gregory & Taylor, 1981; Gregory & Criss, 1986). Values of $\Delta_{\text{plagioclase-pyroxene}}$ for the Bellevue core samples (and PP27, a norite collected 10 km SE of Sandsloot) are consistent with equilibrium at magmatic temperatures. The norites collected from the hanging wall of the Platreef (with the exception of one sample, PP59) plot on an isotherm (Fig. 8) with a slightly larger value of $\Delta_{\text{plagioclase-pyroxene}}$ (average 2.0‰), which corresponds to a temperature of 512°C [using the equation for $\text{An}_{55}\text{–Di}$ of Chiba *et al.* (1989)]. These data are consistent with oxygen isotope equilibrium between plagioclase and pyroxene persisting to slightly lower temperatures than is normal in the Bushveld. The most likely explanation for this is the presence of fluid during slow cooling. The relatively large difference in bulk $\delta^{18}\text{O}$ value of these norites shows that oxygen isotopes were not homogenized during this process, which is consistent with a relatively low water/rock ratio. It should be noted also that the ferrogabbro sample also has a $\Delta_{\text{plagioclase-pyroxene}}$ value close to 2.0‰ , which is consistent with the alteration event occurring at some later time.

A significant number of pyroxenite samples have plagioclase and pyroxene $\delta^{18}\text{O}$ values that are not consistent with oxygen isotope equilibrium at magmatic temperatures. These pyroxenites form an array that cuts across the isotherms of Fig. 8. As the amount of alteration observed petrographically increases, the $\delta^{18}\text{O}$ value of plagioclase increases and the $\delta^{18}\text{O}$ value of pyroxene decreases. This is contrary to the normal situation in hydrothermally altered layered intrusions (e.g. Taylor & Forester, 1979; Gregory & Criss, 1986; Taylor, 1987). There are two possible explanations for the Platreef pyroxenite data:

(1) the pyroxenites crystallized with a range of $\delta^{18}\text{O}$ values, and the subsequent fluid–rock interaction resulted in shifts to higher $\delta^{18}\text{O}$ value in the plagioclase whereas the pyroxene $\delta^{18}\text{O}$ values remained constant.

(2) Equilibrium was maintained between plagioclase and pyroxene (and their alteration products) during fluid–rock interaction. The value of 3.6‰ for $\Delta_{\text{plagioclase-pyroxene}}$ in sample PP11 would be consistent with a temperature of equilibration between plagioclase and pyroxene of $\sim 300^\circ\text{C}$ (Chiba *et al.*, 1989). However, at these temperatures in the presence of fluid, the pyroxene and plagioclase would have, at least partially, converted to low-temperature hydrous silicates such as chlorite and clay minerals

The montmorillonite–chlorite fractionation factor for oxygen [calculated by combining the chlorite–water and montmorillonite–water equations of Wenner & Taylor (1973) and Sheppard & Gilg (1996)] should approximate the expected fractionation between highly altered plagioclase and pyroxene, and ranges from 0.6‰ at 400°C to 3.3‰ at 200°C . Thus, even at relatively low temperatures, the observed per mil difference between ‘plagioclase’ and ‘pyroxene’ cannot be produced by their alteration to montmorillonite and chlorite, respectively. Explanation (1) is therefore more likely to be correct, with the pyroxenites having a range of pre-alteration $\delta^{18}\text{O}$ values presumably produced by crustal contamination. The modal abundance of plagioclase in these rocks is much less than that of pyroxene and as a result its $\delta^{18}\text{O}$ values would have been much more sensitive to fluid–rock interaction than those of the pyroxene. Again, this suggests that the alteration process is one of low water/rock ratio. Unfortunately, the data do not allow a distinction to be made between the single or multiple intrusion hypotheses for the origin of the norites and pyroxenites.

CONCLUSIONS

(1) Apart from the Platreef, the northern limb has the same oxygen isotope characteristics as the Eastern Limb of the Bushveld. The original magma(s) had $\delta^{18}\text{O}$ values

that are 1–1.5‰ higher than expected in an uncontaminated mantle-derived magma. Archaean granite and lower-crustal granulites do not have high enough $\delta^{18}\text{O}$ values for them to be realistic potential contaminants. We therefore agree with Schiffries & Rye (1989) that contamination by Transvaal Supergroup sedimentary rocks is the most likely cause of these high $\delta^{18}\text{O}$ values. There is no evidence for changes in magma $\delta^{18}\text{O}$ value over a 2500 m section through the upper part of the northern limb. This suggests that intrusion was filled with well-mixed, already contaminated magma(s). The fact that the Transvaal Supergroup sedimentary rocks are the only realistic contaminants implies that the contamination process took place in a magma chamber within the crust.

(2) The Platreef norites and pyroxenites were affected by additional crustal contamination. The most likely contaminant was the country rock dolomite, which forms the footwall at Sandsloot. Simple mixing calculations suggest that the Platreef pyroxenites with the highest $\delta^{18}\text{O}$ values crystallized from magmas that had assimilated 18% dolomite in addition to the earlier contamination by Transvaal Supergroup rocks. Dolomite contamination is unlikely to have resulted in diopside or olivine crystallizing instead of orthopyroxene, or to have affected the trace element or Sr-isotope composition of the Platreef.

(3) It is clear that the rocks within and just above the Platreef were affected by fluid–rock interaction to a much greater degree than in the rest of the intrusion. The Platreef shows both petrographic and oxygen isotope evidence for interaction with an external fluid. This fluid appears to have been magmatic in origin, on the basis of its hydrogen isotope composition and that of apparently associated quartz veins. The fluid both affected the magmatic component of the Platreef and lowered the $\delta^{18}\text{O}$ values of the dolomite within the Platreef and in the immediate footwall. The fluid–rock interaction appears to have taken place at low water/rock ratios.

(4) The lack of disturbance of the Sr-isotope system suggests that the fluid–rock interaction took place soon after intrusion. Hence the alteration of the Platreef did not occur as a response to long-term or much younger fluid movement along the contact between the intrusion and the country rock.

ACKNOWLEDGEMENTS

Financial support for this work was provided by the National Research Foundation. We are indebted to Fay-rooza Rawooot, Fran Pocock, Shireen Govender and Steve Richardson for help with the analytical work. AMPLATS provided access to Sandsloot Mine and gave permission for this paper to be published. The help of the staff of the Geology Department at the Potgietersrus

Platinum Mine is gratefully acknowledged. We also thank Chris Lee of AMPLATS for help in getting the project off the ground, Lew Ashwal for providing material from the Bellevue core, and Marian Tredoux for reading a preliminary version of this manuscript. We are particularly grateful to Grant Cawthorn and Christian Tegner for their many constructive comments on the manuscript. This paper was written while the first author was Professeur Invité at Université Jean Monnet, St-Etienne.

REFERENCES

- Ashwal, L. D. & Hart, R. J. (1995). Trace element geochemistry of Bushveld plagioclases. *Geological Society of South Africa, Centennial Geocongress, Johannesburg*. Johannesburg: Geological Society of South Africa, pp. 492–495.
- Ballhaus, C. & Stumpfl, E. F. (1986). Sulphide and platinum mineralization in the Merensky Reef: evidence from hydrous silicates and fluid inclusions. *Contributions to Mineralogy and Petrology* **94**, 193–204.
- Barker, F., Friedman, I., Hunter, D. R. & Gleason, J. D. (1976). Oxygen isotopes of some trondjemites, siliceous gneisses, and associated mafic rocks. *Precambrian Research* **3**, 547–557.
- Barnes, S. J. & Campbell, I. H. (1988). Role of late magmatic fluids in Merensky-type platinum deposits: a discussion. *Geology* **16**, 488–491.
- Barton, J. M., Jr, Cawthorn, R. G. & White, J. A. (1986). The role of contamination in the evolution of the Plat Reef of the Bushveld Complex. *Economic Geology* **81**, 1096–1104.
- Borthwick, J. & Harmon, R. S. (1982). A note regarding ClF_3 as an alternative to BrF_3 for oxygen isotope analysis. *Geochimica et Cosmochimica Acta* **46**, 1665–1668.
- Boudreau, A. E. & McCallum, I. S. (1992). Concentration of platinum-group elements by magmatic fluids in layered intrusions. *Economic Geology* **87**, 1830–1848.
- Buchanan, D. L., Nolan, J., Suddaby, P., Rouse, J. E., Viljoen, M. J. & Davenport, J. W. J. (1981). The genesis of sulphide mineralisation in a portion of the Potgietersrus limb of the Bushveld Complex. *Economic Geology* **76**, 568–579.
- Cartwright, I. & Buick, I. S. (1999). The flow of surface-derived fluids through Alice Springs age middle-crustal ductile shear zones, Reynolds Range, central Australia. *Journal of Metamorphic Geology* **17**, 397–414.
- Cawthorn, R. G., Barton, J. M., Jr & Viljoen, M. J. (1985). Interaction of floor rocks with the Platreef on Overysel, Potgietersrus, northern Transvaal. *Economic Geology* **80**, 988–1006.
- Chacko, T., Mayeda, T. K., Clayton, R. N. & Goldsmith, J. R. (1991). Oxygen and carbon isotope fractionation between CO_2 and calcite. *Geochimica et Cosmochimica Acta* **55**, 2867–2882.
- Chiba, H., Chacko, T., Clayton, R. N. & Goldsmith, J. R. (1989). Oxygen isotope fractionations involving diopside, forsterite, magnetite, and calcite: applications to geothermometry. *Geochimica et Cosmochimica Acta* **53**, 2985–2995.
- Clayton, R. N., O'Neil, J. R. & Mayeda, T. K. (1972). Oxygen isotope exchange between quartz and water. *Journal of Geophysical Research* **77**, 3057–3067.
- Coplen, T. B., Kendall, C. & Hoppo, J. (1983). Comparison of stable isotope reference samples. *Nature* **302**, 236–238.
- Craig, H. (1961). Isotopic variations in meteoric waters. *Science* **133**, 1702–1703.

- Davies, G., Cawthorn, R. G., Barton, J. M. & Morton, M. (1980). Parental magma to the Bushveld Complex. *Nature* **287**, 33–35.
- Deer, W. A., Howie, R. A. & Zussman, J. (1992). *An Introduction to the Rock-forming Minerals*. Harlow: Longman, 696 pp.
- DePaolo, D. J. (1981). Trace element and isotopic effects of combined wall rock assimilation and fractional crystallisation. *Earth and Planetary Science Letters* **53**, 189–202.
- Duncan, A. R., Erlank, A. J. & Betton, P. J. (1984). Appendix 1: analytical techniques and data base descriptions. *Geological Society of South Africa, Special Publication* **13**, 389–395.
- Eales, H. V. & Cawthorn, R. G. (1996). The Bushveld Complex. In: Cawthorn, R. G. (ed.) *Layered Intrusions*. Amsterdam: Elsevier, pp. 181–229.
- Faure, K. & Harris, C. (1991). Oxygen and carbon isotope geochemistry of the 3·2 Ga Kaap Valley tonalite, Barberton greenstone belt, South Africa. *Precambrian Research* **52**, 301–319.
- Gain, S. B. & Mostert, A. B. (1982). The geological setting of the platinoïd and base metal sulfide mineralisation in the Platreef of the Bushveld Complex in Drenthe, north of Potgietersrus. *Economic Geology* **77**, 1395–1404.
- Giletti, B. J. (1986). Diffusion effects on oxygen isotope temperatures of slowly cooled igneous and metamorphic rocks. *Earth and Planetary Science Letters* **77**, 218–229.
- Gregory, R. T. & Criss, R. E. (1986). Isotopic exchange in open and closed systems. In: Valley, J. W., Taylor, H. P., Jr & O'Neil, J. R. (eds) *Stable Isotopes in High Temperature Geological Processes*. Mineralogical Society of America, *Reviews in Mineralogy* **16**, 91–127.
- Gregory, R. T. & Taylor, H. P., Jr (1981). An oxygen isotope profile in a section of Cretaceous oceanic crust, Samail ophiolite, Oman: evidence for $\delta^{18}\text{O}$ buffering of the oceans by deep (>5 km) seawater–hydrothermal circulation at mid-ocean ridges. *Journal of Geophysical Research* **86**, 2737–2755.
- Gregory, R. T., Criss, R. E. & Taylor, H. P., Jr (1989). Oxygen isotope exchange kinetics of mineral pairs in closed and open systems: applications to problems of hydrothermal alteration of igneous rocks and Precambrian iron formations. *Chemical Geology* **75**, 1–42.
- Hamilton, J. (1977). Strontium isotope and trace element studies on the Great Dyke and Bushveld mafic phase and their relation to early Proterozoic magma genesis in southern Africa. *Journal of Petrology* **18**, 24–52.
- Harmer, R. E. & Sharpe, M. R. (1985). Field relations and strontium isotope systematics of the marginal rocks of the eastern Bushveld Complex. *Economic Geology* **80**, 813–837.
- Harris, C. & Erlank, A. J. (1992). The production of large-volume low- $\delta^{18}\text{O}$ rhyolites during the rifting of Africa and Antarctica: the Lebombo Monocline, southern Africa. *Geochimica et Cosmochimica Acta* **56**, 3561–3570.
- Hattingh, P. J. (1983). A palaeomagnetic investigation of the layered mafic sequence of the Bushveld complex. Ph.D. thesis, University of Pretoria.
- Ito, E., White, W. M. & Gopel, C. (1987). The O, Sr, Nd, and Pb isotope geochemistry of MORB. *Chemical Geology* **62**, 157–176.
- James, D. E. (1981). The combined use of oxygen and radiogenic isotopes as indicators of crustal contamination. *Annual Review of Earth and Planetary Sciences* **9**, 311–344.
- Knoper, M. W. & von Gruenewaldt, G. (1992). Main Zone parental magma composition in the northern Bushveld Complex, Potgietersrus: evidence from REE content of plagioclase (abstract). *Geological Society of South Africa, 24th Geocongress, Bloemfontein*. Johannesburg: Geological Society of South Africa, p. 237.
- Kruger, F. J. & Marsh, J. S. (1982). The significance of $^{87}\text{Sr}/^{86}\text{Sr}$ ratios in the Merensky cycle of the Bushveld Complex. *Nature* **298**, 53–55.
- Kyser, T. K., O'Neil, J. R. & Carmichael, I. S. E. (1981). Oxygen isotope thermometry of basic lavas and mantle xenoliths. *Contributions to Mineralogy and Petrology* **77**, 11–23.
- La Grange, M. S., Stevens, G. & Harris, C. (2000). Metamorphism of Witwatersrand rocks in the collar of the Vredefort structure: a petrographic and O isotope study. *Journal of African Earth Sciences* **31**, 39–40.
- Lee, C. A. (1996). A review of mineralization in the Bushveld Complex and some other layered intrusions. In: Cawthorn, R. G. (ed.) *Layered Intrusions*. Amsterdam: Elsevier, pp. 103–145.
- Le Maitre, R. W. (1989). *A Classification of Igneous Rocks and Glossary of Terms*. Oxford: Blackwell.
- Mathez, E. A., Agrinier, P. & Hutchinson, R. (1994). Hydrogen isotope composition of the Merensky Reef and related rocks, Atok Section, Bushveld Complex. *Economic Geology* **89**, 791–802.
- Mattey, D., Lowry, D. & Macpherson, C. (1994). Oxygen isotope composition of mantle peridotites. *Earth and Planetary Science Letters* **128**, 231–241.
- McCrea, J. M. (1950). On the isotopic chemistry of carbonates and a paleotemperature scale. *Journal of Chemical Physics* **18**, 849–857.
- Nell, J. (1985). The Bushveld Metamorphic Aureole in the Potgietersrus area: evidence for a two-stage metamorphic event. *Economic Geology* **80**, 1129–1152.
- O'Neil, J. R. (1986). Theoretical and experimental aspects of isotopic fractionation. In: Valley, J. W., Taylor, H. P., Jr & O'Neil, J. R. (eds) *Stable Isotopes in High Temperature Geological Processes*. Mineralogical Society of America, *Reviews in Mineralogy* **16**, 1–40.
- Reid, D. L., Cawthorn, R. G., Kruger, F. J. & Tredoux, M. (1993). Isotope and trace-element patterns below the Merensky Reef, Bushveld Complex, South Africa: evidence for fluids? *Chemical Geology (Isotope Geosciences Section)* **106**, 171–186.
- SACS (South African Committee on Stratigraphy) (1980). *Stratigraphy of South Africa. Geological Survey of South Africa, Handbook* **8**, 690 pp.
- Schiffries, C. M. & Rye, D. M. (1989). Stable isotopic systematics of the Bushveld Complex: I. Constraints of magmatic processes in layered intrusions. *American Journal of Science* **289**, 841–873.
- Schiffries, C. M. & Rye, D. M. (1990). Stable isotope systematics of the Bushveld Complex: II. Constraints on hydrothermal processes in layered intrusions. *American Journal of Science* **290**, 209–245.
- Sharpe, M. R. (1981). The chronology of magma influxes to the eastern compartment of the Bushveld Complex as exemplified by its marginal border groups. *Journal of the Geological Society, London* **138**, 307–326.
- Sheppard, S. M. F. (1996). Characterization and isotopic variation in natural waters. In: Valley, J. W., Taylor, H. P., Jr & O'Neil, J. R. (eds) *Stable Isotopes in High Temperature Geological Processes*. Mineralogical Society of America, *Reviews in Mineralogy* **16**, 165–183.
- Sheppard, S. M. F. & Gilg, H. A. (1996). Stable isotope geochemistry of clay minerals. *Clay Minerals* **31**, 1–24.
- Tankard, A. J., Jackson, M. P. A., Eriksson, K. A., Hobday, D. K., Hunter, D. R. & Minter, W. E. L. (1982). *Crustal Evolution of South Africa—3·8 Billion Years of Earth History*. New York: Springer, pp. 175–199.
- Taylor, B. E. (1986). Magmatic volatiles: isotopic variation of C, H, and S. In: Valley, J. W., Taylor, H. P., Jr & O'Neil, J. R. (eds) *Stable Isotopes in High Temperature Geological Processes*. Mineralogical Society of America, *Reviews in Mineralogy* **16**, 185–225.
- Taylor, H. P., Jr (1968). The oxygen isotope geochemistry of igneous rocks. *Contributions to Mineralogy and Petrology* **19**, 1–71.
- Taylor, H. P., Jr (1977). Water/rock interactions and the origin of H_2O in granitic batholiths. *Journal of the Geological Society, London* **133**, 509–558.
- Taylor, H. P., Jr (1980). The effects of assimilation of country rocks by magmas on $^{18}\text{O}/^{16}\text{O}$ and $^{87}\text{Sr}/^{86}\text{Sr}$ systematics in igneous rocks. *Earth and Planetary Science Letters* **47**, 243–254.

- Taylor, H. P., Jr (1987). Comparison of hydrothermal systems in layered gabbros and granites, and the origin of low- ^{18}O magmas. In: Mysen, B. O. (ed.) *Magmatic Processes: Physicochemical Principles. Geochemical Society Special Publication 1*, 337–357.
- Taylor, H. P., Jr & Forester, R. W. (1979). An oxygen and hydrogen isotope study of the Skaergaard intrusion and its country rocks: a description of a 55-M.y. old fossil hydrothermal system. *Journal of Petrology* **20**, 355–419.
- Taylor, H. P., Jr & Sheppard, S. M. F. (1986). Igneous rocks. I. Processes of isotopic fractionation and isotope systematics. In: Valley, J. W., Taylor, H. P., Jr & O'Neil, J. R. (eds) *Stable Isotopes in High Temperature Geological Processes. Mineralogical Society of America, Reviews in Mineralogy 16*, 227–271.
- Valley, J. W. (1986). Stable isotope geochemistry of metamorphic rocks. In: Valley, J.W., Taylor, H.P., Jr & O'Neil, J.R. (eds) *Stable Isotopes in High Temperature Geological Processes. Mineralogical Society of America, Reviews in Mineralogy 16*, 445–489.
- Van der Merwe, M. J. (1976). The layered sequence of the Potgietersrus limb of the Bushveld Complex. *Economic Geology* **71**, 1337–1351.
- Vennemann, T. W. & O'Neil, J. R. (1993). A simple and inexpensive method of hydrogen isotope and water analyses of minerals and rocks based on zinc reagent. *Chemical Geology (Isotope Geosciences Section)* **103**, 227–234.
- Vennemann, T. W. & Smith, H. S. (1990). The rate and temperature of reaction of ClF_3 with silicate minerals, and their relevance to oxygen isotope analysis. *Chemical Geology* **86**, 83–88.
- Wagner, P. A. (1925). Notes on the platinum deposits of the Bushveld Igneous Complex. *Transactions of the Geological Society of South Africa* **27**, 83–133.
- Walraven, F., Armstrong, R. A. & Kruger, F. J. (1990). A chronostratigraphic framework for the north-central Kaapvaal craton, the Bushveld Complex and the Vredefort structure. *Tectonophysics* **171**, 23–48.
- Wenner, D. B. & Taylor, H. P., Jr (1973). Oxygen and hydrogen isotope studies of the serpentinization of ultramafic rocks in oceanic environments and continental ophiolite complexes. *American Journal of Science* **273**, 207–239.